



HAL
open science

Recent Advances in Hydrodeoxygenation of Lignin-Derived Phenolics over Metal-Zeolite Bifunctional Catalysts

Ping He, Lin Li, Yuanchao Shao, Qisong Yi, Zhifeng Liu, Huawei Geng,
Yuanshuai Liu, Valentin Valtchev

► **To cite this version:**

Ping He, Lin Li, Yuanchao Shao, Qisong Yi, Zhifeng Liu, et al.. Recent Advances in Hydrodeoxygenation of Lignin-Derived Phenolics over Metal-Zeolite Bifunctional Catalysts. ChemCatChem, inPress, 10.1002/cctc.202301681 . hal-04650618

HAL Id: hal-04650618

<https://hal.science/hal-04650618v1>

Submitted on 16 Jul 2024

HAL is a multi-disciplinary open access archive for the deposit and dissemination of scientific research documents, whether they are published or not. The documents may come from teaching and research institutions in France or abroad, or from public or private research centers.

L'archive ouverte pluridisciplinaire **HAL**, est destinée au dépôt et à la diffusion de documents scientifiques de niveau recherche, publiés ou non, émanant des établissements d'enseignement et de recherche français ou étrangers, des laboratoires publics ou privés.

Recent Advances in Hydrodeoxygenation of Lignin-Derived Phenolics over Metal-Zeolite Bifunctional Catalysts

Ping He,^{1,3,4} Lin Li,^{1,3,4,6} Yuanchao Shao,^{1,3,4} Qisong Yi,^{1,3,4,5} Zhifeng Liu,^{1,3,4} Huawei Geng,^{1,3,4} Yuanshuai Liu,^{1,3,4,*} Valentin Valtchev^{1,2,*}

¹Qingdao Institute of Bioenergy and Bioprocess Technology, Chinese Academy of Sciences, Songling Road 189, Laoshan District, Qingdao, 266101, China.

²Laboratoire Catalyse et Spectrochimie, Normandie Univ, ENSICAEN, UNICAEN, CNRS, 6 boulevard Maréchal Juin, 14050 Caen, France.

³Shandong Energy Institute, Songling Road 189, Laoshan District, Qingdao, 266101, China.

⁴Qingdao Energy Shandong Laboratory, Songling Road 189, Laoshan District, Qingdao, 266101, China.

⁵University of Chinese Academy of Sciences, 19A Yuquan Road, Shijingshan District, Beijing, 100049, China.

⁶College of Chemistry and Chemical Engineering, Ocean University of China, Songling Road 238, Laoshan District, Qingdao, 266101, China.

Abstract: The hydrodeoxygenation (HDO) reaction provides a promising catalytic strategy to remove oxygen in biomass-derived bio-oil to produce renewable transportation fuels and value-added chemicals. The development of highly efficient and stable HDO catalysts plays an essential role in biomass valorization. Metal-zeolite bifunctional catalysts have been well-developed as the effective HDO catalysts in upgrading lignin-derived phenolics due to their excellent activity, selectivity, and thermal and hydrothermal stability. However, clarifying the roles of the active sites and their synergistic effect, and establishing effective structure-performance relationships in the HDO process still face challenges. In this review, we first survey the conventional catalysts applied in the HDO of bio-oil, followed by thoroughly discussing the roles of metal centers, acid sites, supports, and their impacts on the HDO process of phenolic model compounds or bio-oil. Finally, a discussion on the stability and deactivation of metal-zeolite catalysts, especially in the aqueous-phase HDO reaction, is provided. This critical review offers new insights into the development of state-of-the-art metal-zeolite bifunctional catalysts with well-defined porosity and metal-acid properties for viable biomass valorization.

Keywords: Biomass; Hydrodeoxygenation; Bifunctional catalyst; Zeolites; Catalyst rational design

1. Introduction

The increasing concern about climate change forces us to pursue a sustainable carbonaceous resource instead of fossil resources to produce fuels, chemicals and functional materials. The use of biomass, the abundant and only renewable organic carbon resource on Earth, is regarded as an effective route to produce those fossil-derived energy and materials in the context of carbon neutrality without hazardous environmental effects.^[1-2] Among the various biomass, lignocellulose, commonly found in grass, wood, straw and their solid wastes, represents more than 90% of all plant biomass. Consequently, the value-added use of lignocellulose has attracted much attention in the past decades.^[3]

Lignocellulose is composed of cellulose, hemicellulose and lignin (Figure 1). As the most abundant component in lignocellulosic biomass, cellulose is a linear polymer with glucose units linked via β -1-4 glycosidic bonds.^[4-5] Unlike cellulose, hemicellulose is an amorphous branched polymer consisting of five- and six-carbon polysaccharide units.^[6-7] Lignin is another amorphous polymer consisting of three major phenylpropane units/hydroxyl cinnamyl alcohols such as p-hydroxyphenyl (H), guaiacyl (G) and syringal units (S) bonded through β -O-4, α -O-4, 5-5, β -5, and other linkages.^[8-9] The proportion of three components in lignocellulose depends on the feedstock and are approximately cellulose (40-45 wt%), hemicellulose (25-35 wt%), and lignin (20-30 wt%). In general, biomass refinery using lignocellulose as feedstock can be proceeded through thermal, biological, chemical, or mechanical processes, which have been developed over the last several decades.^[10-11] Due to their relatively simple structures, cellulose and hemicellulose have been maturely applied to produce sugars, ethanol, and other biofuels via hydrolysis or the cascade catalysis processes. Unlike the carbohydrate part of lignocellulose, lignin is often considered as a low-value residue, traditionally either released as waste or burnt to generate heat and sometimes power. Therefore, how to transform lignin, the largest renewable source of aromatic building blocks in nature, into more diverse and valuable products determines the profitability and sustainability of current biorefineries with the

utilization of whole biomass.^[12]

Thermochemical/thermocatalytical transformation of lignocellulosic biomass generally involves gasification, pyrolysis, and hydrothermal liquefaction. Among those techniques, fast pyrolysis represents an industrially attractive and efficient technology for the conversion of lignocellulose into bio-oil, which is a complex mixture of hundreds of different organic compounds, including phenolics, alkanes, furans, ethers, carboxylic acids, aldehydes, ketones, etc. (Figure 1).^[13-16] The quantity and quality of the bio-oil depend on the chemical composition of biomass, thermochemical conversion approach, and the operating conditions. However, the obtained primary bio-oil cannot be directly used as a transportation fuel because of its deleterious properties such as low calorific value, low stability, high polarity, easy-to-coke, and causticity towards equipment. All those shortages of bio-oil are attributed to its high oxygen content. Therefore, reducing oxygenated compounds in crude bio-oil is the key to bio-oil upgrading.

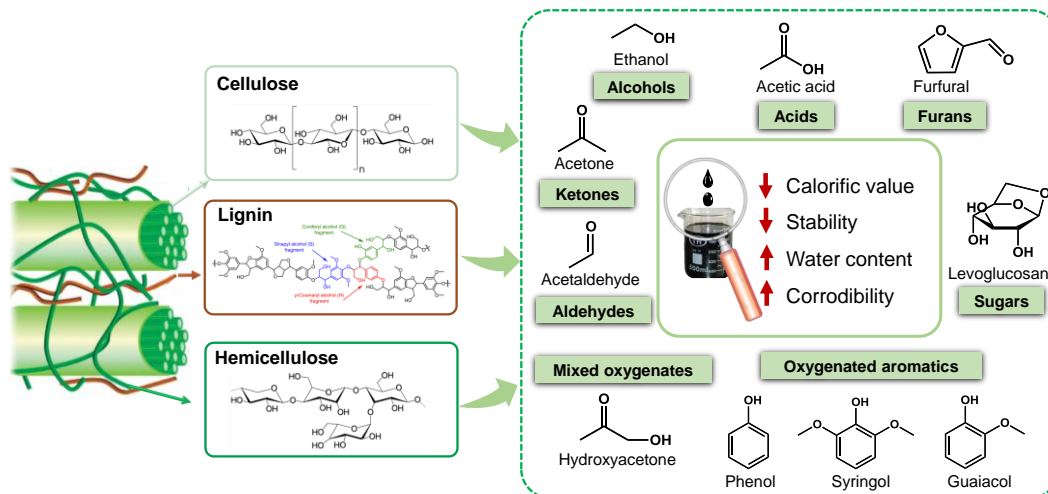


Figure 1. Three major components in lignocellulose and their structural units, as well as the compounds present in pyrolysis bio-oil from lignocellulosic biomass.

Taking the lignin-derived phenolic bio-oil for example, hydrotreatment, cracking, steam reforming, etc., have been recognized as effective approaches decreasing the oxygen content.^[17-18] Among them, hydrodeoxygenation (HDO) is able to enhance the calorific value by increasing H/O ratios in organic compounds, offering a promising

pathway to upgrade phenolic oil to fuels and value-added chemicals. In general, the catalytic HDO of phenolics involves a range of reactions including hydrogenation, hydrogenolysis, dehydration, isomerization and alkylation. From a mechanistic point of view, there are two main reaction pathways for catalytic HDO of phenolics, i.e., hydrogenation-deoxygenation (HYD) and direct deoxygenation (DDO). In the HYD process, the hydrogenation of aromatic ring in phenolics first occurs, followed by the elimination of $C_{alkyl}\text{-OH}$ via dehydration without any carbon loss.^[19-20] In DDO, the oxygen in the form of $C_{aryl}\text{-OH}$ or $C_{aryl}\text{-OCH}_3$ group attached to the aromatic ring can be directly removed by C-O bond scission via hydrogenolysis.^[21] The HYD/DDO ratio determines the distribution of overall products, which relies largely on the catalyst employed, reaction conditions and feedstock composition.^[22-24]

Bifunctional catalysts containing a combination of acidity (active for elimination and alkylation) and a metal phase (active for hydrogenation and hydrogenolysis) appear to be the most beneficial for the HDO of phenolics, and have received much attention in recent years.^[25-26] Scheme 1 depicts the possible HDO reaction pathways of guaiacol, a representative phenolic compound derived from lignin, over metal-acid bifunctional catalysts.^[27] The oxygen removal of guaiacol over metal active sites primarily proceeds through the hydrogenolysis and hydrogenation steps. In the presence of acid sites, acid-catalyzed dehydration of alcohols ($C_{alkyl}\text{-OH}$ bond scission) and alkylation reactions (including C-C and C-O bond formation) occur, resulting in a complex reaction network. Owing to the diversity of reactions and complex components in lignin-derived phenolics, catalytic roles of bifunctions and their synergistic effect during the HDO still require in-depth research before they are still not completely understood. In this contribution, we review the upgrading of bio-oil via the HDO process, focusing on bifunctional metal-acid catalysts. The nature and structure of catalytic active sites, the properties of support, and the relationship between catalyst and HDO performance (activity, selectivity and stability) will be discussed. This review aims to provide a guidance for the rational design of new or better catalysts for the bifunctionally catalyzed HDO of lignin-derived phenolic bio-oil.

catalytic activity than traditional sulfide catalysts in HDO reaction, especially Ni₂P catalysts.^[37-38] The good performance of Ni₂P is attributed to its higher d-electron density and a combination of structural and electronic influences of phosphorus atoms on the transition metal sites, which favors the adsorption of oxygenated compounds and C-O bond cleavage. However, this kind of catalyst still needs to be further improved due to its poor stability in the presence of water at high temperatures. Carbide and nitride catalysts (e.g., Mo₂C, Mo₂N) which are known as “quasi noble metal catalysts” also show high activity in phenolic HDO reactions similar to the conventional metal sulfide and noble metal catalysts.^[39] Nevertheless, carbides and nitrides are prone to oxidation, leading to a decline in HDO reactivity and changed product selectivity associated with the enhanced acidity by oxygen passivation. Therefore, further research is needed to improve the stability and selectivity of these catalysts, paving the way for their applications in bio-oil upgrading.

As a main component of heterogeneous catalysts, the support plays important roles, such as improving the metal dispersion, enhancing the catalyst stability against metal aggregation and leaching, offering the second functionality of acidity or basicity, etc. Many kinds of supports, including alumina, silica, active carbon, TiO₂, ZrO₂ and zeolite, have been used for HDO reactions.^[40-45] Zeolites with high-surface area, unique shape selectivity, adjustable acidity and robust thermal/hydrothermal stability have been widely used as catalysts and acidic supports for petroleum refining and bio-oil upgrading.^[46-49] As a bifunctional catalyst, metal supported over acidic zeolites is easier to realize the HDO of phenolics toward target hydrocarbons via a hydrogenation-dehydration-hydrogenation route in a cascade mode.^[50-51] For example, in the HDO of guaiacol, Pt/Al-MCM-48 with a high quantity of acid sites showed a relatively high guaiacol conversion, whereas Pt/Si-MCM-48 with no acid sites led to a negligible guaiacol conversion.^[52] Similar results in the HDO of anisole showed that Pt/Al₂O₃ could give 100% conversion of m-cresol with a high selectivity to methylcyclohexanol at 150 °C under 2 MPa of H₂, while Pt/HBEA (Pt supported on H-type Beta zeolite) could reach complete conversion of m-cresol to 99% methylcyclohexane under the same reaction conditions.^[53] Other studies also confirm

that the metal phase in metal-acid bifunctional catalysts could activate C=C and C=O bonds towards hydrogenation, and the acid phase could promote dehydration, hydrocracking and isomerization, collaboratively resulting in the complete deoxygenation of refractory phenolic derivatives.^[54-56] Even though the acidic zeolite-supported metal catalysts show remarkable activity in HDO of phenolic compounds and have received much attention, clarifying the role of different active sites and their cooperative effects during the reactions is still challenging with regard to the rational design of high-efficiency HDO catalysts.

2.1 The role of metal active sites

Metal-acid-catalyzed HDO of phenolics usually involves a combination of diversity reactions, such as hydrogenation, hydrogenolysis, decarbonylation, dehydration, alkylation, etc., often resulting in a wide range of product distribution. Thus, it is necessary to develop a proper catalyst with optimized selectivity in target products. In general, hydrogenation is much easier to occur over metals because of its low activation barriers.^[57-59] In contrast, deoxygenation appears relatively hard to occur due to high energy requirement for C-O bond cleavage, which is also regarded as the rate-determining step in HDO reactions.^[60] When acidic zeolite is applied as a support, the specific pore architectures of zeolites can facilitate steric adsorption and selective transformation of molecules, thereby delivering unique shape selectivity for the target product. Meanwhile, the synergistic effects of bifunctionalities, particularly within the confinement microenvironment, could significantly enhance the HDO performance, improve the catalyst stability, and even open new reaction pathways.^[27, 54-56]

Noble metal-based catalysts (e.g., Pd, Pt, Ru, Rh) are usually used in HDO of phenolic compounds due to their strong capability to activate hydrogen and conduct hydrogenation reactions under relatively mild conditions.^[61-63] When supported on HBEA zeolites with comparable metal loading, the HDO activity of lignin-derived phenolics followed the order of Rh/HBEA > Ru/HBEA > Pt/HBEA > Pd/H-BEA. Meanwhile, for selectivity towards the desired product (cyclohexanol), the order was

observed as Ru/HBEA > Pt/HBEA > Rh/HBEA > Pd/H-BEA.^[64] As substitutes for noble metal catalysts, non-noble metal catalysts including Ni, Fe, Cu, etc., have received significant attention in the hydrogenation or deoxygenation of phenolic compounds.^[65-67] According to the first-principle density functional theory (DFT) calculations, Co, Mo, Ni, and Cu showed higher adsorption energies of anisole than other metals such as Mn, Fe, Zn, Ru, Rh, Pd, and Pt, implying the strong binding between anisole and the surface of those non-noble metal species, which was of importance to determine their catalytic activity.^[66] In the HDO of m-cresol, the hydrogenation of the carbonyl group was found to follow the order of Pd > Ni > Ru > Cu under reaction conditions of atmospheric H₂ pressure and temperature of 350 °C, leading to the formation of toluene as the major product.^[67] Although many supported noble and non-noble metal catalysts have been investigated for HDO of phenolics, it is still very hard to directly compare the variety of different catalysts tested under varying reaction conditions.

Figure 2a summarizes the selectivity of deoxygenated products when feeding vapor-phase aromatic oxygenates such as cresol or guaiacol.^[54] The reaction pathway of HDO that occurs over a given transition metal depends on how strongly it binds oxygen. Metals like Pt and Pd can form relatively weak metal-oxygen bonds, and the decarbonylation via C-C scission is often a dominant pathway for oxygen removal. While on Fe and Ni, C-O bond scission is often favored because of the formation of stronger metal-oxygen bonds. This suggests that deoxygenation of phenolic bio-oil may be best accomplished using a bifunctional catalyst that combines hydrogenation sites with sites that form strong metal-oxygen bonds.

In addition to the type of metals, the loading, particle size and dispersion of the metal species are crucial factors influencing their catalytic activity and the selectivity of final products. For example, Ni₂P supported over a hierarchical ZSM-5 zeolites (Ni₂P/h-ZSM-5) catalysts with Ni loadings of 2.5-10 wt% were prepared and tested for the HDO of m-cresol.^[68] The dispersion of Ni₂P was inversely proportional to Ni loading, and exhibited structure-sensitivity with small particles (< 7 nm) offering higher turnover frequencies (TOFs) (Figure 2b). In general, the particle size of the

metal determines its surface structures, i.e., concentrations of terrace, step, corner, and kink sites. These sites may show different activities due to their different abilities in molecule adsorption and bond formation/breaking resulting from their variable local environment.^[69-70] Mortensen et al. investigated the influence of nickel particle size (5-22 nm) for the liquid-phase HDO of phenol over Ni/SiO₂ catalysts and observed a strong particle size effect on hydrogenation and deoxygenation reactions (Figure 2c).^[71] In detail, they found that the hydrogenation rate increased with increasing Ni particle size while the opposite trend was observed for the deoxygenation step. In the vapor-phase HDO of m-cresol, Zhu and coworkers demonstrated that surface Ni atoms on smaller particles were more active than those in larger ones. The smaller particles with more defect sites (step and corner) favored deoxygenation and hydrogenation while larger particles with more terrace sites favored C-C hydrogenolysis.^[72]

Although non-noble metal catalysts have low prices, they usually require relatively high loadings to achieve the desired activity compared to the noble metal catalysts. The use of them as a second metal to form bimetallic catalysts with other metals is one of the effective approaches to strengthen their HDO activity.^[73-74] For example, RuCo bimetallic catalyst presented a strong interaction between two metals, which led to higher adsorption of hydrogen and substrate onto the catalyst and, thereby, an improved HDO performance of guaiacol with a high yield of hydrocarbon products.^[75] A similar study reported that introducing Fe into Pd could result in the modification of the electronic properties of Pd by electron transfer from Fe to Pd, leading to an enhanced catalytic activity.^[76] Bimetallic MoW carbide catalysts exhibited a much higher density of H₂-activating sites than those monometallic catalysts, giving high activity and a completely deoxygenated product with selectivity of 92 mol% in the HDO of guaiacol.^[77] In Fe-Ni/HZSM-5 catalyst, the addition of Fe not only increased the dispersion of NiO, but also enhanced the adsorption of hydrogen and promoted C=O hydrogenation in Ni-Fe bimetallic catalysts, which jointly resulted in the improved HDO performance of pine sawdust bio-oil.^[78]

To demonstrate the deoxygenation efficiency and understand the fundamental

effect of the second metal on bimetallic catalysts, two series of bimetallic catalysts Ni-Cu/HZSM-5 and Ni-Co/HZSM-5 were tested in the HDO of phenol.^[79] As shown in Figure 2d, the modification of Ni/HZSM-5 catalysts with Cu significantly deteriorated the catalytic performance. In contrast, an admixture of Co increased the activity and selectivity toward the target hydrocarbons of benzene and cyclohexane. In Ni-Co/HZSM-5 catalysts, cobalt could increase nickel dispersion and reduce particle size, giving 99 % hydrocarbon selectivity at complete phenol conversion and a significantly reduced coke deposition.

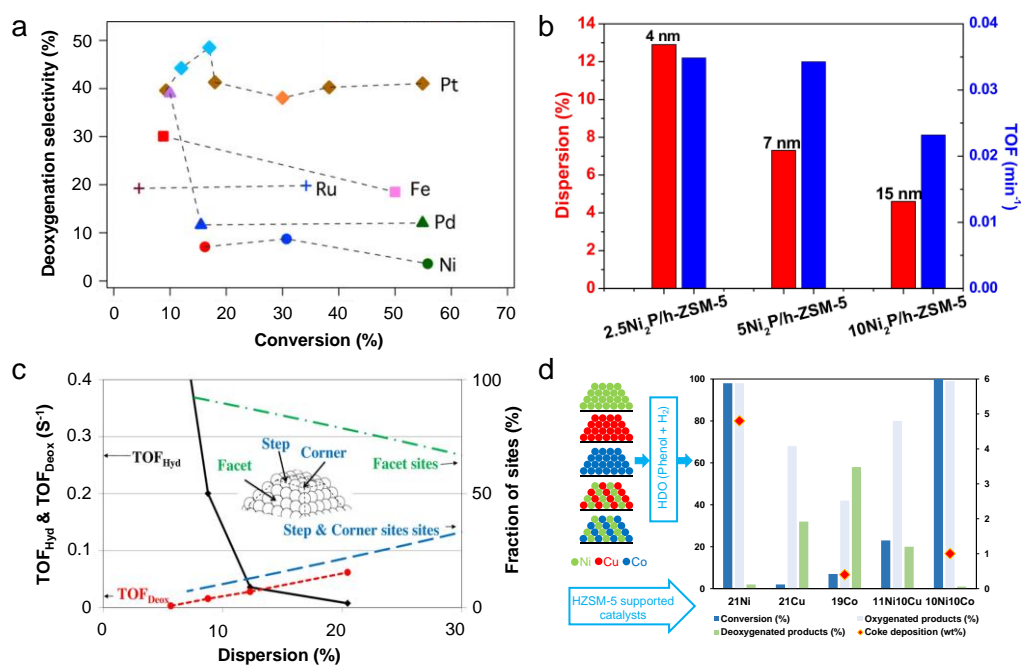


Figure 2. (a) Selectivity to deoxygenated products from feeding aromatic oxygenates (cresol or guaiacol) over Pt (diamonds), Ru (crosses), Fe (squares), Pd (triangles), and Ni (circles) catalysts. Reproduced from ref. [54]. Copyright (2016), with permission from American Chemical Society. (b) Correlation between turnover frequency for HDO of *m*-cresol and active phase dispersion of Ni₂P/h-ZSM-5 catalysts. Reproduced from ref. [68]. Copyright (2018), with permission from Elsevier. (c) Turnover frequency for hydrogenation (TOF_{Hyd}) and deoxygenation (TOF_{Deox}) over Ni/SiO₂ catalysts as a function of metal dispersion, and the fraction of sites as a function of dispersion. Reproduced from ref. [71]. Copyright (2016), with permission from Elsevier. (d) The catalytic activity, product distribution, and coke deposition of monometallic and bimetallic catalysts in the HDO of phenol. Reproduced from ref. [79]. Copyright (2014), with permission from Wiley-VCH.

As suggested above, a bifunctional catalyst that combines hydrogenation sites with sites that can form strong metal-oxygen bonds would be helpful to the

deoxygenation of phenolic compounds. Oxophilic metals, such as Cu, Fe, Zn, and Co, favor the adsorption of O atom and facilitate the C-O and C=O bonds cleavage, thus enabling the deoxygenation activity.^[73, 80-81] That means those oxophilic metals could be used as the second metal added to the noble metal-based catalyst. The noble metals can activate hydrogen, and the oxophilic metals can strongly bind the reactant to the surface through the M-O bond, resulting in an easier C-O scission and potentially creating new reaction pathways which are unavailable on a monometallic catalyst.

2.2 The role of support

Supports are typically used for loading and dispersing active components, and play an important role in the adsorption and activation of reaction substrates. Moreover, supports with specific acidity are beneficial for oxygen removal via elimination steps during HDO of phenolic compounds. Therefore, the specific surface area, pore structure, and acid-base properties of the support, as well as the interaction between the support and metal components, are important for the dispersion, particle size distribution, and electronic structure of metal active components, and thereby affect the catalytic performance of the catalyst.

The characteristic high surface area of zeolites allows them to host metal species with good dispersion and form highly active bifunctional catalysts. The introduction of mesopores affected Ni dispersion and particle size, which subsequently determined the effectiveness of the catalyst.^[82] Self-pillared nanosheet ZSM-5 with highly exposed surface areas could improve the dispersion of Pt-Ni alloy on its surface by establishing strong metal-support interaction, promoting the adsorption and spillover of hydrogen, and thus giving an enhanced HDO activity of phenolics (Figure 3a).^[83] Besides, it was found that the Rh dispersion increased with increasing $S_{\text{ext}}/S_{\text{BET}}$ ratio of the support.^[84] Moreover, the supports could affect the chemical states of metal species. For example, Ni₃P, Ni₁₂P₅, and Ni₂P were the major crystal phases when SiO₂ and HZSM-5 were used as support, while nickel metal rather than nickel phosphides was generated on Al₂O₃.^[85] This was probably due to the interaction of Al₂O₃ with phosphorous species during high-temperature calcination. Among three catalysts,

Ni₃P/HZSM-5, a bifunctional catalyst with hydrogenation and acid sites, showed the highest HDO activity of phenol (Figure 3b).

For a specific reaction, the reactants first adsorb on the catalysts' surface and the reactants' adsorption mode could largely determine their reaction pathways. Two major adsorption modes of phenolic compounds have been reported on the surface of the catalyst, i.e., coordination adsorption and coplanar adsorption, which would affect the reaction pathway of HDO. In detail, coordination adsorption favors the DDO reaction of phenolics, while coplanar adsorption favors the HYD reaction.^[19] Sievers et al. found that the yield of deoxygenation product over Pt/HBEA was in the order of anisole > m-cresol > guaiacol.^[86] The reactivity difference of the three molecules was caused by their different adsorption manner, where the type and position of functional groups play an important role. Anisole and m-cresol can form phenate and cresolate surface species after adsorbing on the Lewis acid sites of HBEA. In contrast, guaiacol can adsorb more strongly by forming bidentate catecholate or methoxy phenate species, which might hamper its mass transport during reactions.

In HDO of phenol, Cao et al. proposed a new methodology to facilitate benzene formation rather than hydrogenation of phenyl with minimized H₂ consumption by hindering the adsorption of phenyl.^[87] At elevated temperature, hydrogenation of phenyl was dramatically inhibited via decreased adsorption of benzene ring than that of hydroxyl, thus favoring hydrogenolysis over hydrogenation reaction in parallel mode. Zhu et al. also reported that the direct deoxygenation of phenolics to aromatics dominated the HDO path at ambient H₂ pressure and higher temperatures over Pt/HBEA catalysts.^[88-90] The aromatics may be produced from the fast dehydrogenation of cyclohexenes, which is thermodynamically favored at high temperatures. Similarly, Minoru et al. modified the surface of the Pt/HZSM-5 catalyst by using ionic liquids to increase the selectivity to aromatics in the HDO of phenolics at atmospheric pressure of H₂.^[91] Unmodified Pt/HZSM-5 converted phenolics into aliphatic species as the major products. In contrast, arenes' selectivity over the modified catalyst could reach up to 76% (Figure 3c). The ionic liquids may offer the adsorption of phenols in an edge-to-face manner onto the surface, thus accelerating

the HDO without ring hydrogenation. Therefore, the reaction activity and products distribution could be tailored by controlling the adsorption mode of oxygenated compounds in the HDO process.

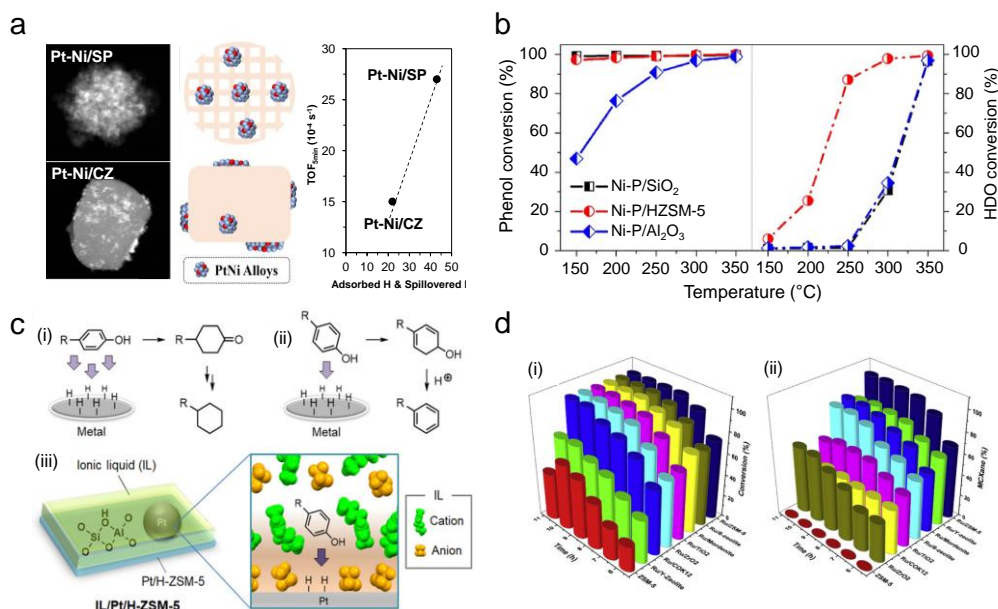


Figure 3. (a) HAADF-STEM images of Pt-Ni/SP (Pt-Ni supported over self-pillared nanosheet ZSM-5 zeolite) and Pt-Ni/CZ (Pt-Ni supported over commercial microporous ZSM-5 zeolite), and the relation between H species (adsorption and spillover) and TOF values on two catalysts. Reproduced from ref. [83]. Copyright (2022), with permission from Elsevier. (b) Phenol conversion and HDO conversion over three Ni-P catalysts with different supports in the aqueous phase. Reproduced from ref. [85]. Copyright (2019), with permission from Elsevier. (c) Presumed adsorption modes of phenols onto a metal surface forming: (i) aliphatics and (ii) arenes, and (iii) schematic images for the surface structure of ionic liquids modified Pt/HZSM-5 (IL/Pt/H-ZSM-5) in the HDO of phenols. Reproduced from ref. [91]. Copyright (2019), with permission from Wiley-VCH. (d) The impact of support on the HDO of m-cresol: (i) conversion of m-cresol, (ii) selectivity of methylcyclohexane. Reproduced from ref. [95]. Copyright (2020), with permission from Elsevier.

Supports with certain acidity are beneficial for the HDO activity of the catalyst. The type, concentration, and strength of acid sites, are closely related to the activity of the catalyst.^[92-93] Solid acids such as Al₂O₃ and zeolites are the commonly used acidic supports in deoxygenation catalysts since many studies have shown their superiority in catalyzing oxygen removal from biomass pyrolysis oil.^[94-96] To investigate the support effects in HDO reaction, Ru supported on various acidic solids including ZSM-5, Mordenite, Beta zeolite, Y zeolite, TiO₂, ZrO₂, and COK12 were tested for

HDO of m-cresol to methylcyclohexane.^[95] All catalysts showed 100% conversion except Ru/Y (72%) due to the high concentration of acid sites on Y zeolite which would cause coke formation and rapidly deactivation of the catalyst. The selectivity of methylcyclohexane followed the order of Ru/ZSM-5 > Ru/Mordenite > Ru/Beta > Ru/Y. The results revealed that the product selectivity was determined by both acidity and pore structure of the support (Figure 3d). Similarly, Ga-supported catalysts were tested for HDO of m-cresol, and the toluene yield followed the order of Ga/SiO₂ < Ga/HZSM-5 < Ga/HBEA.^[49] The Ga/HBEA was the most active catalyst, although its acidity was weaker than that of Ga/HZSM-5. The higher activity of Ga/HBEA was attributed to the less restrictions of m-cresol diffusion within the larger pores of BEA zeolite. Besides the acidity, the support pore size significantly affects the deoxygenation of biomass-derived bulky molecules.

2.2.1 The acidity of support

In the HDO of phenolics, support with certain acidity can promote the dehydration of alcohol intermediates produced by the ring hydrogenation. Too weak acid sites might be unable to attract oxygen from the oxygenated compounds. At the same time, very strong acidity tends to cause severe cracking or an alkylation reaction, leading to coke deposition and deactivation of catalysts. For instance, γ -Al₂O₃ is usually used as the support of HDO catalysts at an early study stage.^[40, 97] However, too strong Lewis acidity makes it prone to form carbon deposition on its surface. Additionally, γ -Al₂O₃ can be easily converted into AlOOH under hydrothermal conditions, resulting in poor stability with structural collapse and deactivation.^[98] In comparison, supports with less acidity or basicity (SiO₂ or MgO) show their advantages in deferring the coke formation in HDO reactions.^[99-100]

Brønsted and Lewis acid sites usually play different roles in upgrading bio-oil. In the HDO of guaiacol, the presence of Brønsted acid sites provided by zeolites can effectively facilitate the conversion of 2-methoxycyclohexanol to cyclohexane. Conversely, catalysts such as Ru/Al₂O₃ and Ru/SiO₂, which solely possess weak Lewis acidity without any Brønsted acid functionality, showed limited deoxygenation

activity.^[101] In the HDO of p-cresol, it was also concluded that Brønsted acid sites can serve as adsorption sites for oxygen atoms from p-cresol and supply protons to the hydroxyl group of p-cresol, thereby weakening C_{aryl}-OH bonds and significantly enhancing the HDO activity. In contrast, Lewis acidic support such as Al₂O₃ and other metal oxides exhibited negligible promotion effect.^[102] Nevertheless, the additional Lewis acid sites may facilitate the catalytic reaction by binding the oxygenated substrates and subsequently cleaving the C-O linkages.^[103]

The rates of the sequential reactions involved in HDO of phenol were compared over Ni-supported HZSM-5 and Al₂O₃-HZSM-5 catalysts. Ni/Al₂O₃-HZSM-5 showed up to five times higher catalytic activity for phenol hydrogenation than Ni/HZSM-5 and delivered higher rates for overall phenol HDO, which was attributed to the Lewis acidity introduced by Al₂O₃ binder that could stabilize a ketone intermediate and inhibited its hydrogenation.^[104] Similarly, the mixed catalysts Ni/Al-HZSM-5 exhibited the maximum phenol conversion of 99.6% with the highest cyclohexane selectivity of 98.3%, which can be partially attributed the stronger acid sites and synergistic effect of Brønsted and Lewis acidities (Figure 4a).^[105] Besides, Ni₂P loaded catalysts showed good HDO activity, since the incorporation of Ni₂P led to an increase in the overall acidity, including both new Lewis (Ni^{δ+} species) and Brønsted acid sites (P-OH groups).^[106-107] The respective roles of Brønsted acid sites and Lewis acid sites on supports were also investigated by employing Ni-supported NaZSM-5, HZSM-5 and Silicalite-1 catalysts. As shown in Figure 4b, except for hydrogenolysis occurred over Ni, the removal of methoxy functional group from 2-methoxy-4-propylcyclohexanol could be catalyzed by Brønsted acid sites. In addition, Brønsted acid sites showed superior activity over Lewis acid sites in the dehydration of 4-propyl-cyclohexanol.^[108]

addition, Ni@ZSM-5-50 catalyst with a high concentration of Lewis acid sites was found to give cyclohexane (via hydrogenation and deoxygenation) as the final product with yield of 91.6% in the HDO of anisole (Figure 5c). While over Ni@ZSM-5-100 with a reduced Lewis acidity, methoxycyclohexane formed through hydrogenation could easily desorb from zeolite surface.^[110]

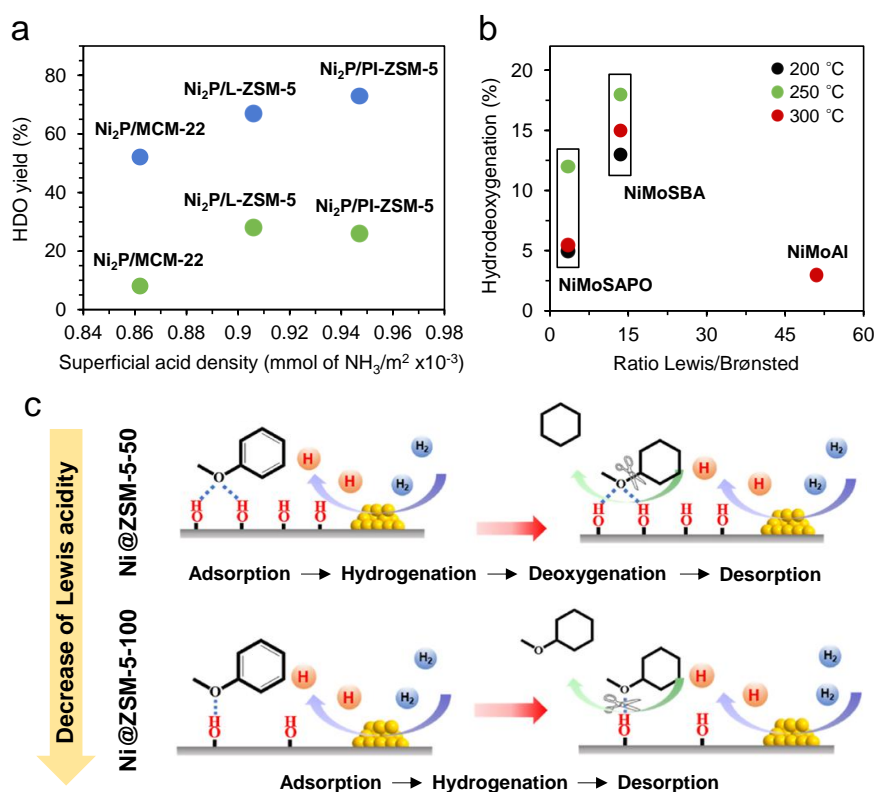


Figure 5. (a) Relationship between the yield of completely deoxygenated compounds at 220 °C (green) and 260 °C (blue) and the surface density of acid sites. Reproduced from ref. [106]. Copyright (2020), with permission from Elsevier. (b) Effect of the ratio of Lewis/Brønsted sites in the HDO of anisole for NiMo catalysts. Reproduced from ref. [110]. Copyright (2018), with permission from Elsevier. (c) Schematic transformation of anisole by Ni@ZSM-5 catalysts with changed Lewis acidity. Reproduced from ref. [111]. Copyright (2022), with permission from Elsevier.

In the HDO of raw bio-oil, it was also demonstrated that the acidity of zeolites affected products distribution and also coke formation. FeMoP supported on HY catalyst with the stronger acidity (compared with HBEA and HZSM-5) could promote dehydration and condensation reactions, significantly increased the water and coke content in the product.^[112] In the HDO of guaiacol, Ru supported over ZSM-5 and BEA zeolites with varying Si/Al ratios were studied. With decreasing the Si/Al ratio of zeolites, the yield of cyclohexane increased, while a decrease in the yield of

2-methoxycyclohexanol was observed. Additionally, both Ru/BEA and Ru/ZSM-5 with low Si/Al ratios displayed high activity in the HDO of guaiacol.^[101]

2.2.2 The porosity of support

Porosity and nanostructure are the most versatile features of heterogeneous solid catalysts, which can greatly determine the accessibility of specific active sites, reaction mechanisms, and the selectivity of desirable products. The zeolites' porosity significantly affects the shape selectivity and the dispersion of metal centers, which could simultaneously improve the catalytic performance of the catalyst. In the HDO of phenolic monomers to alkanes over metal-zeolite catalysts, monocycloalkanes are the main product when using a small pore zeolite such as HZSM-5, while bicycloalkanes can be selectively produced when using a larger pore zeolite such as HY and HBEA as the support.^[113-114] Lee et al. studied the effect of pore size on HDO of guaiacol over Pt/HZSM-5 and Pt/HY.^[115] Although the acidity of Pt/HY was lower, guaiacol conversion over Pt/HY was 5 times higher than that on Pt/HZSM-5, since Pt/HY (supercages with 1.2 nm in diameter and an open aperture of 0.74 nm) could provide sufficient space for the reaction of guaiacol (kinematic diameter: 0.67 nm) compared to Pt/HZSM-5 (0.51 nm × 0.55 nm & 0.53 nm × 0.56 nm). Additionally, zeolites with different topological structures and porosity could also affect the particle size and dispersion of metals in the metal-zeolite bifunctional catalyst.^[27, 116-118]

Although the use of zeolites as solid acids and supports for metallic species is a promising way to design catalysts with high selectivity and stability for the upgrading of bio-oil, their micropores (less than ~1 nm) are not able to host most bulky biomass-derived reactants, preventing the effective utilization of the metal active sites and acid sites inside zeolite pores.^[119-120] For example, when a medium-pore zeolite (HZSM-5) was applied for the catalytic upgrading of bulky oxygenated compounds such as guaiacol, low activity and fast catalyst deactivation were observed.^[68, 121] This was mainly caused by the limited diffusion of guaiacol inside pores of conventional ZSM-5. Therefore, hierarchical zeolites with larger pore size, and thus more accessibility of active sites, are potential supports for HDO catalysts.

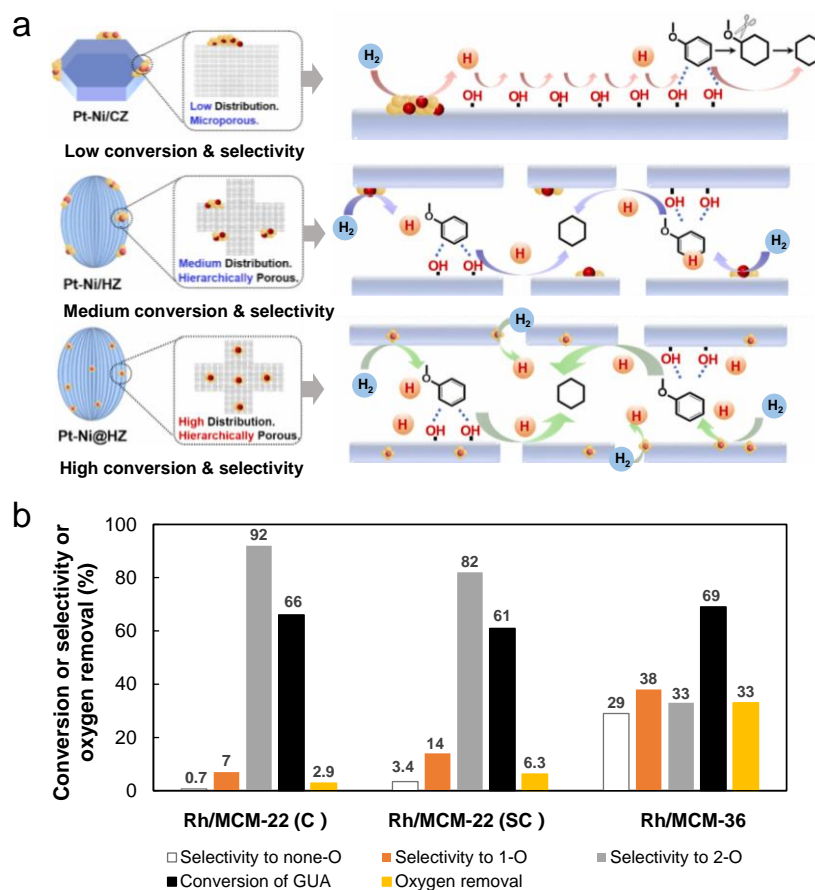


Figure 6. (a) Schematic illustration of the different diffusion pathways and metal dispersion for Pt-Ni bimetals confined in conventional (Pt-Ni/CZ) and hierarchical ZSM-5 zeolite (Pt-Ni/HZ and Pt-Ni@HZ). Reproduced from ref. [122]. Copyright (2023), with permission from Elsevier. (b) HDO reaction of guaiacol on Rh/MCM-22(C), Rh/MCM-22(SC), and Rh/MCM-36 catalysts. Reproduced from ref. [84]. Copyright (2017), with permission from Elsevier.

Hierarchical zeolites possess less diffusional and steric constraints than conventional microporous zeolites. Meanwhile, the hierarchical pore structure also facilitates the dispersion of metal active phase. In the HDO of anisole, the decreased adsorption of anisole as well as the facile aggregation of metal species were observed over conventional ZSM-5 zeolite supported Pt-Ni catalyst (Pt-Ni/CZ), resulting in a reduced catalytic activity (Figure 6a).^[122] When Pt-Ni was supported over a hierarchical ZSM-5 zeolite (i.e., Pt-Ni/HZ and Pt-Ni@HZ in Figure 6a), the larger pore structure facilitated the dispersion of metal species and the adsorption of anisole, as well as the adsorption and spillover of hydrogen, leading to the enhanced HDO of anisole with high selectivity toward cyclohexane. Choi et al. deposited Rh

nanoparticles on MCM-22 zeolite with swollen (MCM-22 (SC)) and pillared (MCM-36) treatment and used them for HDO of 1,3,5-trimethoxybenzene (1,3,5-TMB) and guaiacol.^[84] The results showed that the swelling and pillaring of crystalline MCM-22 zeolites increased the dispersion of Rh metal nanoparticles on the external surface of them compared to pristine MCM-22, and therefore led to the higher HDO activity (Figure 6b).

Nevertheless, the hierarchical pores in zeolites commonly generate undesired framework defects, which would contribute to poor thermal and hydrothermal stability of the catalyst, restricting their practical applications related to the biomass valorization. In addition, it is still very hard to control the mesoporosity of hierarchical zeolite by the conventional desilication or dealumination strategy. Moreover, the metal aggregation under harsh synthesis and reaction conditions would be inevitable even though the diffusion has been facilitated for hierarchical zeolites.^[123] Thus, preparing hierarchical zeolites with properly interconnected channels and uniform metal distribution is still challenging. Recently, zeolites with nanoscale crystal size, such as nanocrystals and nanosheets with intercrystalline pores connected with microporous channels, have shown their potential to alleviate diffusion limitations of macromolecules during reactions.^[124-125] Encapsulation of metal species in single-crystalline nanosheets can be very effective for tuning the selectivity of microporous channels, the fast diffusion of reactive molecules, as well as the high stability of metal species.

2.3 Synergistic effect between metal and acid sites

The performance of metal-acid bifunctional catalysts for the HDO of lignin derivatives depends on their intrinsic activity and also their synergistic actions. The total number and relative ratio between metal and acid sites and their spatial distribution on/within the catalyst, determine the catalytic reaction rate and product selectivity. Therefore, catalyst design with a functional balance is crucial for controlling different elemental steps involved in the HDO process. The synergistic effect of metal-acid sites has been proven to be very helpful in improving the HDO

efficiency, which is mainly determined by the nature and distance of metal and acid sites, as well as the integration form of them. In addition, the change of electronic properties of the metal catalyst by surrounding foreign atoms within supports would result in the improved catalytic performance.^[126]

A favorable functional balance between metal and acid sites can be achieved by adjusting the metal:acid sites ratio and controlling the distance between two active sites. In the Pd/HY catalyzed liquid-phase hydroalkylation of *m*-cresol (Figure 7a), the ring saturation in the first step led to the formation of 3-methylcyclohexanone which was further hydrogenated to methylcyclohexanol on the metal function. The acid catalyzed dehydration of alcohol occurred thereafter to form 3-methylcyclohexene, which could readily alkylate the unreacted *m*-cresol to form bicyclic compounds.^[127] If the hydrogenation of C=C bonds in methylcyclohexene on the metal is faster than alkylation on the acid site, the selectivity of hydroalkylation will decrease. As shown in Figure 7b, the selectivity toward alkylation can be greatly enhanced with increasing the $n_{\text{Acid}}/n_{\text{Metal}}$ (n_A/n_M) ratio. However, too few metal atoms would decrease the overall reaction rate since the initial step in the reaction scheme requires hydrogenation. Yan et al. also reported the effect of the functional balance between metal and acid sites over Ni/HBEA catalysts, and found the reaction pathways and product distribution could be tailored by adjusting the Ni to HBEA ratio.^[128]

In addition to the intrinsic properties and relative ratio of metal and acidic sites, the distance and spatial distribution between them also significantly impact the cascade reactions in HDO.^[116,129-130] The "intimacy criterion" has been proposed to describe the distance between different active sites since 1962 and researchers believe that catalytic activity could be enhanced over active sites with a limited distance.^[131] The close proximity between metal and acid sites could favor the rapid transfer and further reaction of intermediate products, which can effectively suppress the side reactions and improve the product selectivity in HDO of phenolics.^[132] However, there should be an optimization point for metal-acid interactions in phenolic. For example, Fang et al. designed three catalysts with a millimeter scale (Pt-A+Z),

microscale (Pt-A@Z) and nanoscale (Pt-A/Z) distances between metal and acid sites by selective deposition of Pt on Al₂O₃-ZSM-5 nanocomposite, and tested them in HDO of eugenol.^[133] As shown in Figure 7c, the catalytic performances were improved when the distance of metal and acid decreased from millimeter to nanoscale. Pt-A/Z catalysts successfully integrated the (de)hydrogenation ability of metal and deoxygenation activity of zeolites. However, further reducing the distance did not have any influence on the catalytic activity. Moreover, the well-controlled distance between metal nanoparticles and acid centers could remarkably enhance the coke resistance of the catalyst due to the easily transfer of intermediate molecules between the acid sites and metal nanoparticles during the reactions.^[134]

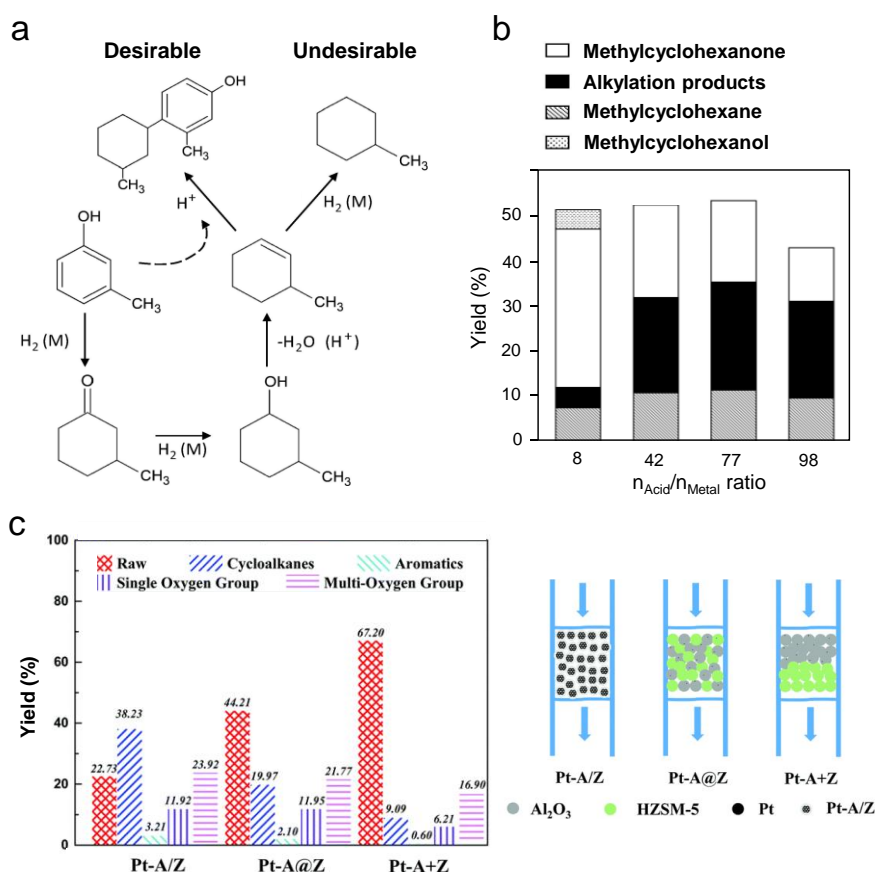


Figure 7. (a) Proposed reaction pathway for HDO and hydroalkylation of m-cresol over Pd/HY catalyst, and (b) the effect of acid/metal ratio on selectivity of alkylated products. Reproduced from ref. [127]. Copyright (2015), with permission from Elsevier. (c) Chemical composition of liquid obtained after HDO of eugenol over the three catalytic system with different metal-acid distances. Reproduced from ref. [133]. Copyright (2018), with permission from Royal Society of Chemistry.

Zhu et al. compared the HDO of guaiacol over HBEA, Pt/SiO₂, and Pt/HBEA at

350 °C under atmospheric pressure, and studied the synergistic effect between acid and metal sites.^[135] The close proximity of Pt and acid sites in bifunctional Pt/HBEA enhanced transalkylation and deoxygenation reactions while inhibited demethylation and decarbonylation reactions significantly, which finally led to aromatics as the major products. Recently, we also found that the effective encapsulation of Ru metal clusters in ITQ-1 and HMCM-22 zeolite cavities could deliver a synergistic effect, leading to an enhanced catalytic activity and product selectivity in the HDO of guaiacol.^[27] Thus, for a new or better HDO catalyst development, more attention must be paid to properly combining metal and acid sites in zeolite with an optimal site ratio and distance.

2.4 Catalyst stability

Unlike industrial operations, the extremely low concentration of biomass-derived model compounds with a high amount of catalyst, together with a short reaction time, were often applied in most of the fundamental studies, thereby the stability of catalysts was always ignored. From an industrial perspective, it is highly necessary to understand the deactivation mechanism of the catalyst used for HDO reaction of bio-oil in order to design an effective and stable catalyst. Generally, there are several reasons for deactivation of metal-zeolite catalyst during HDO process: metal sintering or leaching, coking through carbon deposition, degradation of support, as well as the change in acid sites of zeolite (Figure 8).^[46, 136-137]

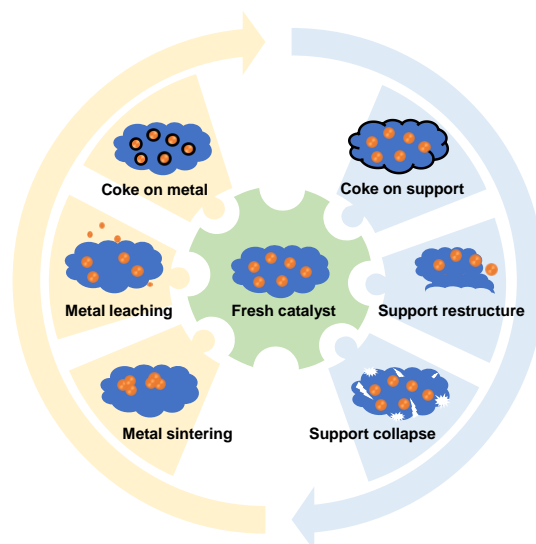


Figure 8. Schematic illustration of the deactivation modes for metal supported catalysts during the HDO processes.

2.4.1 Metal sintering or leaching

The deactivation of the metal phase in metal-zeolite catalysts can be influenced by many different factors, including the type, content, size and distribution of the metal, as well as their interactions with the support. Specifically, sintering and leaching can lead to irreversible catalyst deactivation due to the permanent changes in metal structure and content, while deactivation caused by carbon deposition can be reversed by burning the carbon species deposited on the metal surface in the presence of air or oxygen.

In general, sintering easily occurs at the catalyst with high metal loadings, or under harsh treatment and reaction conditions (high temperature and acidic/alkaline medium), as well as the lack of strong interaction between metal species and the support. In the liquid-phase reaction, the aggregation of metal nanoparticles would become more severe at higher temperatures and in more acidic reaction media, especially for the metal particles located on the external surface of zeolite. For example, the particle size of noble metals such as Pt, Pd, Ru, and Rh, were found to increase obviously under temperatures higher than 200 °C for continuous reaction time, resulting in the decreased catalytic activity.^[138-140]

Leaching is the dissolution of metal active sites into the reaction medium, which can cause seriously catalyst deactivation, and also the products separation and

purification issues.^[141] Metals' leaching depends on the nature of reaction medium (pH, oxidation potential, chelating properties), and bulk or surface properties of metal. In general, base metals are more prone to leaching compared to noble metals. For example, significant Ni leaching was observed in the acidic and chelating reaction media during the aqueous-phase hydrogenation of glucose, whereas Ru catalysts under the same conditions showed higher specific activity and durability with no detectable leaching.^[142]

The stability of metals against sintering and leaching is often correlated to the synthesis methods and post-synthetic modifications of the catalysts.^[143-146] Compared to the traditional method (e.g., impregnation) which is inclined to generate metal species on the external surface of zeolites, the encapsulation of metals in zeolite pores is regarded as an effective approach to alleviate the sintering and leaching issues of metal-zeolite catalysts. Ru metal particles located inside the zeolite by in-situ synthesis method is more resistant to sintering owing to the spacial constraint of zeolite pores, while metal located on the external surface of zeolite tends to form big particles under the same reaction conditions in the liquid phase.^[27] In addition, the stability of metal active sites could be improved through tuning the electronic or geometric properties by adding second metal species.^[147-148]

2.4.2 Coking

One of the major problems inhibiting the large-scale operation of HDO process is the formation of coke. Both the light and the heavy components in bio-oil contributed to the formation of coke during the HDO of bio-oil, especially the heavy components as they could encounter the steric hindrance for accessing the metal sites on the surface of the catalyst.^[149] In the HDO of biomass-derived compounds, two major types of coke are commonly formed. One is oxygen containing hydrogen rich coke, whose O atom can adsorb easily on strong Brønsted acid sites in zeolites and Lewis acid sites in oxophilic metal oxides.^[129, 135, 150-151] The other type of coke is hydrogen deficient graphite-like coke, which is normally formed due to the overreactions or side reactions.^[129, 135] Compared to the oxygenated coke which is loose and easy to be

removed, the graphite-like coke is much denser and difficult to be removed.

Polymerization of unsaturated compounds, especially the oxygen-containing molecules such as phenolics, has been considered as the main cause for formation of coke during the HDO process. The polymerization of the heavy or light species of bio-oil relates to the properties of catalysts, the configuration of the reactor, and the conditions for the process.^[152] During the HDO of bio-oil over Ni-Cu/HZSM-5 and Ni/HZSM-5 catalysts, the soluble coke was found to generate on the surface of Brønsted acid sites via the polymerization of oxygenates in bio-oil.^[153] In addition, the carbocation species generated upon the Brønsted acid sites, such as the dehydration of alcohol intermediates in the cascade HDO process, also contributed significantly to the coke formation. With the progress of the HDO, the soluble coke could be further converted into the disordered graphite-like coke.

An understanding of the deactivation mechanism will be critical to the development of suitable catalysts and optimization of reaction and catalyst regeneration processes. Sievers et al. monitored via operando transmission FTIR spectroscopy the formation and evolution of surface species over Pt/HBEA during HDO of bio-oil model compounds including anisole, m-cresol, and guaiacol, and concluded that coke formation is only one of several factors contributing to the deactivation of zeolites in HDO (Figure 9a).^[86] The formation of relatively small amounts of graphitic coke and polynuclear aromatics could lead to the pronounced deactivation of the zeolite catalysts. In the HDO of phenol over Pd/HY catalyst, it was found that the catalyst acidity is a decisive factor influencing the coke formation (Figure 9b).^[154] Although Pd/HY was an effective catalyst for the HDO of phenol, too high concentration of acid sites could also cause a fast catalyst deactivation due to the coke formation.

One effective solution to prevent coke formation is to tune catalysts' acidity and thus minimize the occurrence of alkylation or polymerization reactions. Another solution could be to use hierarchical zeolite as the support, which could not only allow the reactions with bulky substrates, but may also lead to decreased rates of deactivation caused by the coke deposition (Figure 9c).^[155] The oxidation and/or

reduction treatment of the used catalysts are able to completely/partially regenerate the catalysts by removing the deposited coke, which requires a relatively high thermal stability of the catalyst.^[156] Besides, performing the HDO reaction at moderate conditions such as relatively lower temperatures could be an useful approach to retard coke formation during bio-oil HDO process. In summary, avoiding coke formation requires careful design of the catalyst with balanced hydrogenation/deoxygenation functionalities and finely tuned structure and reaction conditions, which is still an ongoing challenge.^[133, 157]

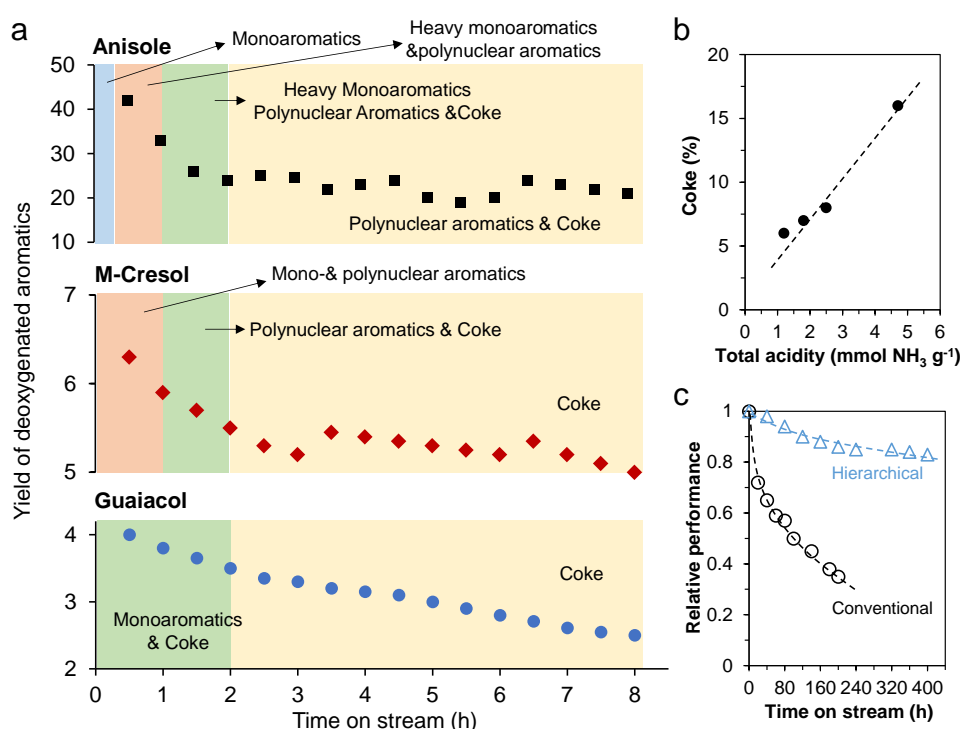


Figure 9. (a) The formation of surface species as a function of time on stream during the HDO of anisole, m-cresol and guaiacol over Pt/HBEA catalyst. Reproduced from ref. [86]. Copyright (2016), with permission from American Chemical Society. (b) Influence of total acidity (determined by NH₃-TPD) on the coke formation in phenol HDO over Pd catalysts supported on mixed HY zeolite and Al₂O₃. Reproduced from ref. [154]. Copyright (2014), with permission from Elsevier. (c) Catalytic activity of conventional and hierarchical Sn-BEA catalysts in the Meerwein-Ponndorf-Verley transfer hydrogenation of cyclohexanone. Reproduced from ref. [155]. Copyright (2016), with permission from Royal Society of Chemistry.

2.4.3 Hydrothermal stability

Water is always involved in the HDO of bio-oil as the reactant or the product,

and in many cases, water has been employed as the solvent. Except for the possible competitive adsorption on active sites, water is also able to oxidize metals and provoke the metal sintering process, resulting in reduced activity.^[158-159] It has been reported that noble metals such as Pt, Pd, and Ru generally have better resistance to sintering and leaching in condensed phase (especially in the aqueous phase) reactions.^[160] Some approaches such as alloying and modification of support, have been applied to enhance the catalysts' HDO activity and structural stability. The coordination between metals, and anchoring the metal on a stable support can be attractive strategies to achieve enhanced catalytic activity and improve hydrothermal stability, attributed to the strong metal-metal and metal-support interactions.^[161-163]

For zeolite support, the hot liquid water greatly impacts their crystallinity, integrity of framework structure and sorption capacity.^[164] It has been proved that the stability of zeolites in hot liquid water highly depends on their framework type, Si/Al ratio, extra-framework cations, and the concentration of silanol defects.^[165-166] For example, zeolites with high framework density, such as MFI and MOR, are relatively stable up to 250 °C, while topologies with low density, such as BEA and FAU, would be destructed at 150 °C. Interestingly, degradation of zeolite could occur in liquid water at high temperatures (> 150 °C), while steaming at the same temperature only limitedly affected the zeolite structure.^[167-168] Wattanakit et al. systematically investigated the stability of Pt-supported HZSM-5 catalysts under hot liquid water, and found that the catalysts exhibit acceptable hydrothermal stability in the temperature range of 50 to 150°C. The catalysts are gradually degraded in the reaction at 150°C for both Pt supported on conventional and hierarchical HZSM-5 due to the loss of relative crystallinity (30-35%).^[169] Čejka and coworkers investigated the effect of hot water at 160 °C for 48h on MWW zeolites, and concluded that the treated MWW zeolites showed less impact on the structure when exposed to water than zeolite BEA.^[170] The structure of all MWW materials was preserved; however, a significant decrease in acid site concentration and micropore volume was observed after hot water treatment.

In the past decade, many useful strategies have been developed to improve the

hydrothermal stability of zeolite-based catalysts. Improving the hydrophobicity of zeolite is one of the most promising strategies to enhance their hydrothermal stability, including surface modification through coating, e.g., with a carbon layer, oxide coating, or anchoring hydrophobic species.^[171-173] Zeolite frameworks typically contain hydrophilic silanol (SiOH) groups, which originate from framework siloxy (i.e., SiO⁻) defects formed during hydrothermal synthesis, and these SiOH species are known to be the main active sites for the hydrolysis of zeolite frameworks in hot liquid water (>150 °C and autogenous pressure).^[174-175] Hence, remediating the negative effect of defects to improve hydrothermal stability of the zeolites, for example, the functionalization of zeolites by silylation approach using organosilane molecules, can be very effective in increasing the hydrophobicity of the material (Figure 10a)^[176-178] and the hydrothermal stability (Figure 10b)^[179]. Another option to improve the stability is doping rare earth cations into the pores of zeolite, which is used to improve thermal stability and increase zeolite structure collapse temperature. For example, the incorporation of Ce can improve the stability of acid centers, but its lower activity was attributed to block or otherwise affect the accessibility of the active sites by the larger size of Ce.^[170] Alternatively, Grand et al. incorporated tungsten in nanosized MFI zeolites to inhibit the formation of silanol defects. The formation of more stable W-O-Si bridges could greatly enhance the structure stability of zeolites.^[180]

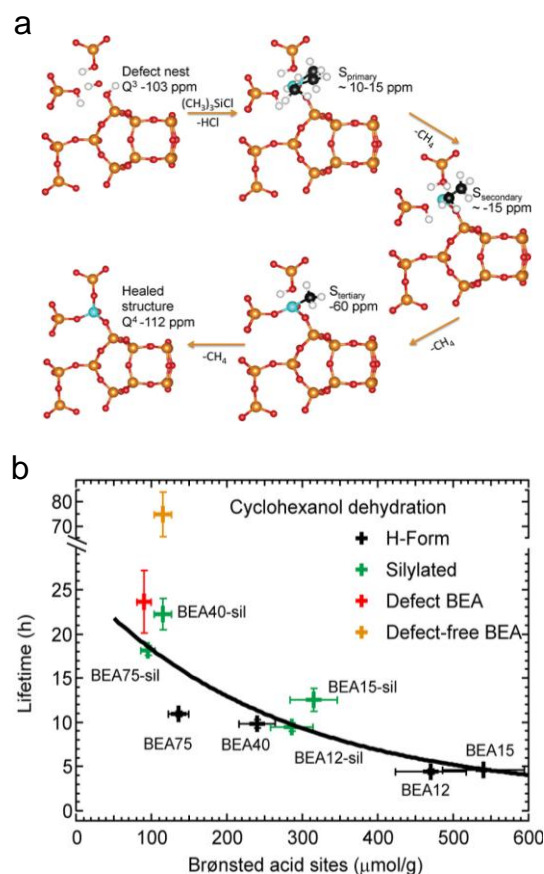


Figure 10. (a) Schematic depiction of a typical silylation procedure for the removal of silanol nests in BEA structure. Reproduced from ref. [177]. Copyright (2016), with permission from American Chemical Society. (b) Correlation between the lifetime and the concentration of Brønsted acid sites of a BEA catalyst during the dehydration of cyclohexanol in the aqueous phase. Reproduced from ref. [179]. Copyright (2017), with permission from American Chemical Society.

3. Summary and perspective

The bifunctionally catalyzed HDO of biomass-derived bio-oil is considered one of the most promising ways to convert biomass into fuels and chemicals. Rational design of highly effective bifunctional catalysts is of great importance for developing HDO processes. Although considerable studies have been performed on various catalysts using model compounds, the difference in chemical properties between bio-crude oil and the model compounds could conceivably lead to suitable catalysts for the model compounds, but ineffective for the bio-crude oil. From the practical standpoint, more attention should be paid to the studies using real or pretreated bio-crude oil as the reactants, paving the way for the truly value-added utilization of biomass resources.

The selection of the metal phase could significantly influence the reaction pathways toward different target hydrocarbons, and metal species with smaller particle sizes and uniform distribution confined in the rigid zeolite matrix are preferred. Appropriate acidic property within zeolites is favorable for C-O cleavage via elimination, and could also inhibit the side reactions of hydro-isomerization and hydrocracking. Zeolite pores provide not only accommodation for metal particles, which is beneficial for its uniform dispersion, but also a confinement space for stabilizing the metal and sometimes reactive intermediates involved in HDO reactions. Hierarchical zeolites with more open structures allow the rapid diffusion of bulky reactants/products and also improve the accessibility of active sites, resulting in enhanced activity as well as a high resistance toward carbon deposition. Although hierarchical or nano-structured zeolites have shown their priority in petrochemical processes, the liquid-phase reaction in biomass valorization could bring additional challenge for zeolite stability since a much more severe destruction of hierarchical structure may occur, especially in hot liquid water. Thus, enhancing the hydrothermal stability of zeolite-based catalysts with an effective and workable approach is highly desired for biomass conversion.

The proper combination of two functional active sites, i.e., metal and acid, has shown its advantages in enhancing reaction rates or selectivity of desired products in HDO of phenolics. Such enhancement was caused by the synergistic effects between two functional sites. However, the underlying mechanism of synergistic effects and an optimal site balance between them, has been limitedly studied. In addition, the lack of effective characterization approaches to monitor the exact state and the nature of active sites under the liquid-phase working conditions leads to difficulties in revealing structure-activity relationships for bifunctional HDO catalysts. Thus, rigorous kinetic studies, advanced characterization techniques, and theoretical calculations should be combined to understand better the synergistic effects between metal and acid in the HDO process. Moreover, designing the catalyst with balanced hydrogenation/deoxygenation functionalities and a finely tuned structure is also important to improve the stability of the HDO catalyst, especially in the presence of a large amount of water

involved in biomass conversion.

Therefore, it is imperative to develop appropriate synthesis methodologies for metal-zeolite bifunctional catalysts that encompass the efficient encapsulation of metal active sites within zeolite pores and precise manipulation of the mesopores and/or nanostructure of zeolites. In addition to the commonly employed impregnation and ion-exchange methods, ligand/polymer-assisted one-pot hydrothermal synthesis routes have emerged as facile strategies for confining metals in zeolites. Multistep post-synthesis techniques, including inter-zeolite framework transformation, two-step dry-gel-conversion, and seed-directing strategies, offer alternative approaches for the preparation of such bifunctional catalysts. To ensure efficient mass transfer of bulky biomass-derived molecules and enhance the accessibility of active sites, it is also essential to fabricate zeolites with mesopores or nanostructures using versatile approaches such as hard-templating, soft-templating, and other post-synthetic treatments.

Overall, applying bifunctional catalysts is an important direction for the HDO of lignin-derived phenolics to fuels and chemicals. Although numerous studies have been devoted to this research area, the rational design of an effective bifunctional catalyst, especially for zeolite-based catalysts, is still a challenging task, which should consider many elements such as porosity and acidity of zeolitic supports, location, particle size, and dispersion of metal centers over zeolitic supports, the balance among metal species, acidity and porosity, and also the thermal and hydrothermal stabilities of active sites and supports. We expect this review is providing valuable guidance for the rational design of new or better catalysts for the bifunctionally catalyzed HDO of lignin-derived phenolic bio-oil.

AUTHOR INFORMATION

Corresponding Author

Yuanshuai Liu; liuys@qibebt.ac.cn

Valentin Valtchev; valentin.valtchev@ensicaen.fr

Author Contributions

The manuscript was written with the contributions of all authors. All authors have approved the final version of the manuscript.

Notes

The authors declare no competing financial interest.

ACKNOWLEDGMENT

The authors acknowledge the start-up fund at Qingdao Institute of Bioenergy and Bioprocess Technology, Chinese Academy of Sciences. Y. Liu acknowledges the support of the National Natural Science Foundation of China (22109167), the Shandong Provincial Natural Science Foundation Project (2022HWYQ-088), and Taishan Scholars Program. P. He acknowledges the Shandong Provincial Natural Science Foundation Project (ZR2022QB110). The authors acknowledge the collaboration in the “Sino-French International Research Network” framework.

References

- [1] F. Shen, X. Xiong, J. Fu, J. Yang, M. Qiu, X. Qi, D. C.W. Tsang, *Renewable Sustainable Energy Rev.*, **2020**, *130*, 109944.
- [2] R. K. Srivastava, N. P. Shetti, K. R. Reddy, E. E. Kwon, M. N. Nadagouda, T. M. Aminabhavi, *Environ. Pollut.*, **2021**, *276*, 116731.
- [3] A. S. Jatoi, S. A. Abbasi, Z. Hashmi, A. K. Shah, M. S. Alam, Z. A. Bhatti, G. Maitlo, S. Hussain, G. A. Khandro, M. A. Usto, A. Iqbal, *Biomass Conv. Bioref.*, **2023**, *13*, 6457-6469.
- [4] A. C. O'sullivan, *Cellulose*, **1997**, *4*, 173-207.
- [5] P. Bajpai, *Pretreatment of lignocellulosic biomass for biofuel production*, **2016**, 7-12.
- [6] Y. Luo, Z. Li, X. Li, X. Liu, J. Fan, J. H. Clark, C. Hu, *Catal. Today*, **2019**, *319*, 14-24.
- [7] C. Bonechi, M. Consumi, A. Donati, G. Leone, A. Magnani, G. Tamasi, C. Rossi, *Bioenergy systems for the future*, **2017**, 3-42.
- [8] M. Li, Y. Pu, A. J. Ragauskas, *Front. Chem.*, **2016**, *4*, 45.
- [9] J. Xu, C. Li, L. Dai, C. Xu, Y. Zhong, F. Yu, C. Si, *ChemSusChem*, **2020**, *13(17)*, 4284-4295.
- [10] P. K. Swain, L. M. Das, S. N. Naik, *Renewable Sustainable Energy Rev.*, **2011**, *15(9)*, 4917-4933.
- [11] A. N. Tabish, M. Kazmi, M. A. Hussain, I. Farhat, M. Irfan, H. Zeb, U. Rafique, H. Ali, M. H. Saddiqi, M. S. Akram, *Waste Biomass Valorization*, **2021**, *12*, 6219-6229.
- [12] C. Chio, M. Sain, W. Qin, *Renewable Sustainable Energy Rev.*, **2019**, *107*, 232-249.
- [13] A.V Bridgwater, *Chem. Eng. J.*, **2003**, *91*, 87-102.
- [14] R. E. Guedes, A. S. Luna, A. R. Torres, *J. Anal. Appl. Pyrolysis*, **2018**, *129*, 134-149.
- [15] Q. Lu, W. Li, X. Zhu, *Energy Convers. Manage.*, **2009**, *50*, 1376-1383.
- [16] W. N. R. W. Isahak, M. W. Hisham, M. A. Yarmo, T. Y. Hin, *Renewable Sustainable Energy Rev.*, **2012**, *16(8)*, 5910-5923.
- [17] S. Xiu, A. Shahbazi, *Renew. Sustain. Energy Rev.*, **2012**, *16(7)*, 4406-4414.
- [18] X. Yue, L. Zhang, L. Sun, S. Gao, W. Gao, X. Cheng, N. Shang, Y. Gao, C. Wang, *Appl. Catal., B*, **2021**, *293*, 120243.
- [19] W. Song, Y. Liu, E. Baráth, C. Zhao, J. A. Lercher, *Green Chem.*, **2015**, *17(2)*, 1204-1218.
- [20] E. Díaz, A. F. Mohedano, L. Calvo, M. A. Gilarranz, J. A. Casas, J. J. Rodríguez, *Chem. Eng. J.*, **2007**, *131*, 65-71.
- [21] M. Shetty, K. Murugappan, T. Prasomsri, W. H. Green, Y. Román-Leshkov, *J. Catal.*, **2015**, *331*, 86-97.
- [22] Z. Luo, Z. Zheng, Y. Wang, G. Sun, H. Jiang, C. Zhao, *Green Chem.*, **2016**, *18*, 5845-5858.
- [23] W. Wan, S. C. Ammal, Z. Lin, K. E. You, A. Heyden, J. G. Chen, *Nat. Commun.*,

2018, *9(1)*, 4612.

- [24] K. Zhang, Q. Meng, H. Wu, J. Yan, X. Mei, P. An, L. Zheng, J. Zhang, M. He, B. Han, *J. Am. Chem. Soc.*, **2022**, *144(45)*, 20834-20846.
- [25] X. Zhang, J. Wu, T. Li, C. Zhang, L. Zhu, S. Wang, *Chem. Eng. J.*, **2022**, *429*, 132181.
- [26] R. A. Rafael, R. Wojcieszak, E. Marceau, F. B. Noronha, *ChemCatChem*, **2023**, *15(18)*, e202300486.
- [27] P. He, Q. Yi, H. Geng, Y. Shao, M. Liu, Z. Wu, W. Luo, Y. Liu, V. Valtchev, *ACS Catal.*, **2022**, *12(23)*, 14717-14726.
- [28] M. Saidi, F. Samimi, D. Karimipourfard, T. Nimmanwudipong, B. C. Gates, M. R. Rahimpour, *Energy Environ. Sci.*, **2014**, *7(1)*, 103-129.
- [29] C. Bouvier, Y. Romero, F. Richard, S. Brunet, *Green Chem.*, **2011**, *13(9)*, 2441-2451.
- [30] C. Dupont, R. Lemeur, A. Daudin, P. Raybaud, *J. Catal.*, **2011**, *279(2)*, 276-286.
- [31] V. Jain, Y. Bonita, A. Brown, A. Taconi, J. C. Hicks, N. Rai, *Catal. Sci. Technol.*, **2018**, *8(16)*, 4083-4096.
- [32] N. Ji, P. Ri, X. Diao, Y. Rong, C. Kim, *Catal. Sci. Technol.*, **2023**, *13(9)*, 2618-2637.
- [33] M. Lang, H. Li, *Fuel*, **2023**, *344*, 128084.
- [34] A. Bjelić, M. Grilc, B. Likozar, *Chem. Eng. J.*, **2020**, *394*, 124914.
- [35] A. S. Ouedraogo, P. R. Bhoi, *J. Cleaner Prod.*, **2020**, *253*, 119957.
- [36] X. Li, G. Chen, C. Liu, W. Ma, B. Yan, J. Zhang, *Renewable Sustainable Energy Rev.*, **2017**, *71*, 296-308.
- [37] V. O.O. Gonçalves, P. M. de Souza, V. T. da Silva, F. B. Noronha, F. Richard, *Appl. Catal. B: Environ.*, **2017**, *205*, 357-367.
- [38] J.-S. Moon, E.-G. Kim, Y.-K. Lee, *J. Catal.*, **2014**, *311*, 144-152.
- [39] M. Zhou, H. A. Doan, L. A. Curtiss, R. S. Assary, *J. Phys. Chem. C*, **2021**, *125(16)*, 8630-8637.
- [40] Z. Yu, Y. Yao, Y. Wang, Y. Li, Z. Sun, Y.-Y. Liu, C. Shi, J. Liu, W. Wang, A. Wang, *J. Catal.*, **2021**, *396*, 324-332.
- [41] Y. Berro, S. Gueddida, S. Lebègue, A. Pasc, N. Canilho, M. Kassir, F. E. H. Hassan, M. Badawi, *Appl. Surf. Sci.*, **2019**, *494*, 721-730.
- [42] W. Jin, J. L. Santos, L. Pastor-Perez, S. Gu, M. A. Centeno, T. R. Reina, *ChemCatChem*, **2019**, *11(17)*, 4434-4441.
- [43] R. Shu, B. Lin, J. Zhang, C. Wang, Z. Yang, Y. Chen, *Fuel Process. Technol.*, **2019**, *184*, 12-18.
- [44] Q. Chen, C. Cai, X. Zhang, Q. Zhang, L. Chen, Y. Li, C. Wang, L. Ma, *ACS Sustainable Chem. Eng.*, **2020**, *8(25)*, 9335-9345.
- [45] Z. Yu, Y. Wang, G. Zhang, Z. Sun, Y.-Y. Liu, C. Shi, W. Wang, A. Wang, *J. Catal.*, **2022**, *410*, 294-306.
- [46] Y. Shi, E. Xing, K. Wu, J. Wang, M. Yang, Y. Wu, *Catal. Sci. Technol.*, **2017**, *7(12)*, 2385-2415.
- [47] B. Valle, R. Palos, J. Bilbao, A. G. Gayubo, *Fuel Process. Technol.*, **2022**, *227*, 107130.

- [48] R. K. Mishra, S. M. Chistie, S. U. Naika, K. Mohanty, *Bioresour. Technol.*, **2022**, 366, 128189.
- [49] A. Ausavasukhi, Y. Huang, A. T. To, T. Sooknoi, D. E. Resasco, *J. Catal.*, **2012**, 290, 90-100.
- [50] W. Luo, W. Cao, P. C. A. Bruijninx, L. Lin, A. Wang, T. Zhang, *Green Chem.*, **2019**, 21(14), 3744-3768.
- [51] Y. Shi, E. Xing, K. Wu, J. Wang, M. Yan, Y. Wu, *Catal. Sci. Technol.*, **2017**, 7(12), 2385-2415.
- [52] E. H. Lee, R. Park, H. Kim, S. H. Park, S.-C. Jung, J.-K. Jeon, S. C. Kim, Y.-K. Park, *J. Ind. Eng. Chem.*, **2016**, 37, 18-21.
- [53] M. J. Watson, *Johnson Matthey Technol. Rev.*, **2014**, 58(3), 156-161.
- [54] A. M. Robinson, J. E. Hensley, J. W. Medlin, *ACS Catal.*, **2016**, 6(8), 5026-5043.
- [55] A. Berenguer, T. M. Sankaranarayanan, G. Gómez, I. Moreno, J. M. Coronado, P. Pizarro, D. P. Serrano, *Green Chem.*, **2016**, 18(7), 1938-1951.
- [56] W. Jiang, J.-P. Cao, J.-X. Xie, L. Zhao, C. Zhang, X.-Y. Zhao, Y.-P. Zhao, and J.-L. Zhang, *Energy Fuels*, **2021**, 35(23), 19543-19552.
- [57] J. Chen, S. Wang, L. Lu, X. Zhang, Y. Liu, *Fuel Process. Technol.*, **2018**, 179, 135-142.
- [58] A. Bakhtyari, A. Sakhayi, M. R. Rahimpour, S. Raeissi, *Int. J. Hydrogen Energy*, **2020**, 45(19), 11062-11076.
- [59] W. Schutyser, G. V. den Bossche, A. Raaffels, S. V. den Bosch, St.-F. Koelewijn, T. Renders, B. F. Sels, *ACS Sustainable Chem. Eng.*, **2016**, 4(10), 5336-5346.
- [60] Z. Si, W. Lv, Z. Tian, K. B. X. Zhang, C. Wang, C. Pang, R. Dong, L. Ma, *Fuel*, **2018**, 233, 113-122.
- [61] J. L. Santos, P. Mäki-Arvela, J. Wärnä, A. Monzón, M. A. Centeno, D. Y. Murzin, *Appl. Catal. B: Environ.*, **2020**, 268, 118425.
- [62] Y. Tian, H. Duan, B. Zhang, S. Gong, Z. Lu, L. Dai, C. Qiao, G. Liu, Y. Zhao, *Angew. Chem. Int. Ed.*, **2021**, 60, 21713-21717.
- [63] W. Zhang, J. Chen, R. Li, S. Wang, L. Chen, K. Li, *ACS Sustainable Chem. Eng.*, **2014**, 2(4), 683-691.
- [64] G. Yao, G. Wu, W. Dai, N. Guan, L. Li, *Fuel*, **2015**, 150, 175-183.
- [65] G. Chen, J. Liu, X. Li, J. Zhang, H. Yin, Z. Su, *Renewable Energy*, **2020**, 157, 456-465.
- [66] J. Zhang, B. Fidalgo, D. Shen, X. Zhang, S. Gu, *Mol. Catal.*, **2018**, 454, 30-37.
- [67] P. Sirous-Rezaei, J. Jae, K. Cho, C. H. Ko, S.-C. Jung, Y.-K. Park, *Chem. Eng. J.*, **2019**, 377, 120121.
- [68] A. Berenguer, J. A. Bennett, J. Hunns, I. Moreno, J. M. Coronado, A. F. Lee, P. Pizarro, K. Wilson, D. P. Serrano, *Catal. Today*, **2018**, 304, 72-79.
- [69] I. M. N. Groot, A. W. Kleyn, L. B. F. Juurlink, *J. Phys. Chem. C*, **2013**, 117, 9266-9274.
- [70] C. A. Teles, N. Duong, R. C. Rabelo-Neto, D. Resasco, F. B. Noronha, *Catal. Sci. Technol.*, **2022**, 12, 5961-5969.
- [71] P. M. Mortensen, J.-D. Grunwaldt, P. A. Jensen, A. D. Jensen, *Catal. Today*, **2016**, 259, 277-284.

- [72] F. Yang, D. Liu, Y. Zhao, H. Wang, J. Han, Q. Ge, X. Zhu, *ACS Catal.*, **2018**, 8(3), 1672-1682.
- [73] H. Wang, H. Ruan, M. Feng, Y. Qin, H. Job, L. Luo, C. Wang, M. H. Engelhard, E. Kuhn, X. Chen, M. P. Tucker, B. Yang, *ChemSusChem*, **2017**, 10(8), 1846-1856.
- [74] B. Chen, F. Li, Z. Huang, G. Yuan, *Appl. Catal. B: Environ.*, **2017**, 200, 192-199.
- [75] R. Shu, R. Li, Y. Liu, C. Wang, P.-F. Liu, Y. Chen, *Chem. Eng. Sci.*, **2020**, 227, 115920.
- [76] J. K. Kim, J. K. Lee, K. H. Kang, J. C. Song, I. K. Song, *Appl. Catal., A*, **2015**, 498, 142-149.
- [77] C.-C. Tran, Y. Han, M. Garcia-Perez, S. Kaliaguine, *Catal. Sci. Technol.*, **2019**, 9, 1387-1397.
- [78] S. Cheng, L. Wei, J. Julson, K. Muthukumarappan, P. R. Kharel, *Fuel Process. Technol.*, **2017**, 167, 117-126.
- [79] T. M. Huynh, U. Armbruster, M.-M. Pohl, M. Schneider, J. Radnik, D.-L. Hoang, B. M. Q. Phan, D. A. Nguyen, A. Martin, *ChemCatChem*, **2014**, 6(7), 1940-1951.
- [80] D. Shi, L. Arroyo-Ramírez, J. M. Vohs, *J. Catal.*, **2016**, 340, 219-226.
- [81] A. M. Robinson, J. E. Hensley, J. W. Medlin, *ACS Catal.*, **2016**, 6(8), 5026-5043.
- [82] D. P. Gamliel, B. P. Baillie, E. Augustine, J. Hall, G. M. Bollas, J. A. Valla, *Microporous Mesoporous Mater.*, **2018**, 261, 18-28.
- [83] L. Guo, Y. Tian, X. He, C. Qiao, G. Liu, *Fuel*, **2022**, 322, 124082.
- [84] J. S. Yoon, T. Lee, J.-W. Choi, D. J. Suh, K. Lee, J.-M. Ha, J. Choi, *Catal. Today*, **2017**, 293, 142-150.
- [85] Z. Yu, A. Wang, S. Liu, Y. Yao, Z. Sun, X. Li, Y. Liu, Y. Wang, D. M. Camaioni, J. A. Lercher, *Catal. Today*, **2019**, 319, 48-56.
- [86] G. S. Foo, A. K. Rogers, M. M. Yung, C. Sievers, *ACS Catal.*, **2016**, 6(2), 1292-1307.
- [87] Y. Shi, E. Xing, J. Zhang, Y. Xie, H. Zhao, Y. Sheng, H. Cao, *ACS Sustainable Chem. Eng.*, **2019**, 7(10), 9464-9473.
- [88] X. Zhu, L. L. Lobban, R. G. Mallinson, D. E. Resasco, *J. Catal.*, **2011**, 281(1), 21-29.
- [89] X. Zhu, L. Nie, L. L. Lobban, R. G. Mallinson, D. E. Resasco, *Energy Fuels*, **2014**, 28(6), 4104-4111.
- [90] Q. Sun, G. Chen, H. Wang, X. Liu, J. Han, Q. Ge, X. Zhu, *ChemCatChem*, **2016**, 8(3), 551-561.
- [91] H. Ohta, K. Tobayashi, A. Kuroo, M. Nakatsuka, H. Kobayashi, A. Fukuoka, G. Hamasaka, Y. Uozumi, H. Murayama, M. Tokunaga, M. Hayashi, *Chem.-Eur. J.*, **2019**, 25(65), 14762-14766.
- [92] F. Broglia, L. Rimoldi, D. Meroni, S. D. Vecchi, M. Morbidelli, S. Ardizzone, *Fuel*, **2019**, 243, 501-508.
- [93] J. Xing, L. Song, C. Zhang, M. Zhou, L. Yue, X. Li, *Catal. Today*, **2015**, 258, 90-95.
- [94] S. Chen, W. Wang, X. Li, P. Yan, W. Han, T. Sheng, T. Deng, W. Zhu, H. Wang, *J. Energy Chem.*, **2022**, 66, 576-586.
- [95] A. Kumar, A. Kumar, B. Biswas, J. Kumar, S. R. Yenumala, T. Bhaskar,

- Renewable Energy*, **2020**, *151*, 687-697.
- [96] Y. Wu, X. Xu, Y. Sun, E. Jiang, X. Fan, R. Tu, J. Wang, *Renewable Energy*, **2020**, *152*, 1380-1390.
- [97] E.-M. Ryymin, M. L. Honkela, T.-R. Viljava, A.O. I. Krause, *Appl. Catal., A*, **2010**, *389(1-2)*, 114-121.
- [98] E. Laurent, B. Delmon, *J. Catal.*, **1994**, *146(1)*, 281-291.
- [99] F. P. Bouxin, X. Zhang, I. N. Kings, A. F. Lee, M. J. H. Simmons, K. Wilson, S.D. Jackson, *Appl. Catal., A*, **2017**, *539*, 29-37.
- [100] J. Zhang, C. Li, X. Chen, W. Guan, C. Liang, *Catal. Today*, **2019**, *319*, 155-163.
- [101] P. Yan, J. Mensah, M. Drewery, E. Kennedy, T. Maschmeyer, M. Stockenhuber, *Appl. Catal., B*, **2021**, *281*, 119470.
- [102] Y. Zhang, T. Liu, H. Jia, Q. Xia, X. Hong, G. Liu, *Catal. Sci. Technol.*, **2022**, *12*, 3426-3430.
- [103] Q. Xia, Z. Chen, Y. Shao, X. Gong, H. Wang, X. Liu, S. F. Parker, X. Han, S. Yang, Y. Wang, *Nat. Commun.*, **2016**, *7*, 11162.
- [104] C. Zhao, S. Kasakov, J. He, J. A. Lercher, *J. Catal.*, **2012**, *296*, 12-23.
- [105] J. Liu, M. Xiang, D. Wu, *Catal. Lett.*, **2017**, *147*, 2498-2507.
- [106] S. Gutiérrez-Rubio, A. Berenguer, J. Přeč, M. Opanasenko, C. Ochoa-Hernández, P. Pizarro, J. Čejka, D. P. Serran, J. M. Coronad, I. Moreno, *Catal. Today*, **2020**, *345*, 48-58.
- [107] V. O.O. Gonçalves, P. M. de Souza, V. T. da Silva, F. B. Noronh, F. Richard, *Appl. Catal., B*, **2017**, *205*, 357-367.
- [108] J. Qi, X. Sun, S.-F. Tang, Y. Sun, C. Xu, X. Li, X. Li, *Appl. Catal., A*, **2017**, *535*, 24-31.
- [109] X. Li, L. Chen, G. Chen, J. Zhang, J. Liu, *Renewable Energy*, **2020**, *149*, 609-616.
- [110] T. L. R. Hwer, A. G. F. Souza, K. T. C. Roseno, P. F. Moreira, R. Bonfim, R. M. B. Alves, M. Schmal, *Renewable Energy*, **2018**, *119*, 615-624.
- [111] S. Li, L. Guo, X. He, C. Qiao, Y. Tian, *Renewable Energy*, **2022**, *194*, 89-99.
- [112] I. Hita, T. Cordero-Lanzac, G. Bonura, C. Cannilla, J. M. Arandes, F. Frusteri, J. Bilbao, *J. Ind. Eng. Chem.*, **2019**, *80*, 392-400.
- [113] C. Zhao, D. M. Camaioni, J. A. Lercher, *J. Catal.*, **2012**, *288*, 92-103.
- [114] C. Zhao, J. A. Lercher, *ChemCatChem*, **2012**, *4(1)*, 64-68.
- [115] H. Lee, H. Kim, M. J. Yu, C. H. Ko, J.-K. Jeon, J. Jae, S. H. Park, S.-C. Jung, Y.-K. Park, *Sci. Rep.*, **2016**, *6(1)*, 28765.
- [116] J. He, Z. Wu, Q. Gu, Y. Liu, S. Chu, S. Chen, Y. Zhang, B. Yang, T. Chen, A. Wang, B. M. Weckhuysen, T. Zhang, W. Luo, *Angew. Chem.*, **2021**, *133(44)*, 23906-23914.
- [117] C. Chen, S. Zhang, Z. Wang, Z.-Y. Yuan, *J. Catal.*, **2020**, *383*, 77-87.
- [118] E. H. Lee, R. Park, H. Kim, S. H. Park, S.-C. Jung, J.-K. Jeon, S. C. Kim, Y.-K. Park, *J. Ind. Eng. Chem.*, **2016**, *37*, 18-21.
- [119] D. Kerstens, B. Smeyers, J. V. Waeyenberg, Q. Zhang, J. Yu, B. F. Sels, *Adv. Mater.*, **2020**, *32(44)*, 2004690.
- [120] D. Xu, H. Lv, B. Liu, *Front. Chem.*, **2018**, *6*, 550.

- [121] L. Wang, J. Zhang, X. Yi, A. Zheng, F. Deng, C. Chen, Y. Ji, F. Liu, X. Meng, F.-S. Xiao, *ACS Catal.*, **2015**, 5(5), 2727-2734.
- [122] Y. Tian, L. Guo, C. Qiao, Z. Sun, Y. Yamauchi, S. Liu, *Appl. Catal., B*, **2023**, 336, 122945.
- [123] Y. Liu, D. Zheng, S. Tao, Y. Lyu, X. Wang, X. Liu, S. Liu, M. Li, R. Zhao, S. Yu, *Catal. Sci. Technol.*, **2021**, 11(14), 4812-4822.
- [124] E. Kianfar, *J. Sol-Gel Sci. Technol.*, **2019**, 91, 415-429.
- [125] N. Wang, Q. Sun, T. Zhang, A. Mayoral, L. Li, X. Zhou, J. Xu, P. Zhang, J. Yu, *J. Am. Chem. Soc.*, **2021**, 143(18), 6905-6914.
- [126] S. J. Tauster, *Acc. Chem. Res.*, **1987**, 20(11), 389-394.
- [127] F. Anaya, L. Zhang, Q. Tan, D. E. Resasco, *J. Catal.*, **2015**, 328, 173-185.
- [128] P. Yan, M. M.-J. Li, E. Kennedy, A. Adesina, G. Zhao, A. Setiawan, M. Stockenhuber, *Catal. Sci. Technol.*, **2020**, 10(3), 810-825.
- [129] X. Wu, Q. Sun, H. Wang, J. Han, Q. Ge, X. Zhu, *Catal. Today*, **2020**, 355, 43-50.
- [130] H. J. Cho, D. Kim, S. Li, D. Su, D. Ma, B. Xu, *ACS Catal.*, **2019**, 10(5), 3340-3348.
- [131] P. B. Weisz, *Adv. Catal.*, **1962**, 13, 137-190.
- [132] Z. Yang, B. Luo, R. Shu, Z. Zhong, Z. Tian, C. Wang, Y. Chen, *Fuel*, **2022**, 319, 123617.
- [133] C. Ju, M. Li, Y. Fang, T. Tan, *Green Chem.*, **2018**, 20(19), 4492-4499.
- [134] S. Xu, J. Du, H. Li, J. Tang, *Ind. Eng. Chem. Res.*, **2018**, 57(42), 14088-14095.
- [135] L. Nie, B. Peng, X. Zhu, *ChemCatChem*, **2018**, 10(5), 1064-1074.
- [136] C. H. Bartholomew, *Appl. Catal., A*, **2001**, 212(1-2), 17-60.
- [137] Y. Wang, G. Wang, L. I. van der Wal, K. Cheng, Q. Zhang, K. P. de Jong, Y. Wang, *Angew. Chem.*, 2021, 133(32), 17876-17884.
- [138] S. E. Wanke, P. C. Flynn, *Catal. Rev.*, **1975**, 12(1), 93-135.
- [139] W. Luo, P. C. A. Bruijninx, B. M. Weckhuysen, *J. Catal.*, **2014**, 320, 33-41.
- [140] D. Gao, C. Schweitzer, H. T. Hwang, A. Varma, *Ind. Eng. Chem. Res.*, **2014**, 53(49), 18658-18667.
- [141] I. Sádaba, M. L. Granados, A. Riisager, E. Taarning, *Green Chem.*, **2015**, 17(8), 4133-4145.
- [142] B. Kusserow, S. Schimpf, P. Claus, *Adv. Synth. Catal.*, **2003**, 345(1-2), 289-299.
- [143] B. Zhang, Q. Wu, C. Zhang, X. Su, R. Shi, W. Lin, Y. Li, F. Zhao, *ChemCatChem*, **2017**, 9(19), 3646-3654.
- [144] N. Wang, Q. Sun, R. Bai, X. Li, G. Guo, J. Yu, *J. Am. Chem. Soc.*, **2016**, 138(24), 7484-7487.
- [145] J. Zhang, L. Wang, B. Zhang, H. Zhao, U. Kolb, Y. Zhu, L. Liu, Y. Han, G. Wang, C. Wang, D. S. Su, B. C. Gates, F.-S. Xiao, *Nat. Catal.*, **2018**, 1(7), 540-546.
- [146] L. Liu, U. Díaz, R. Arenal, G. Agostini, P. Concepción, A. Corma, *Nat. Mater.*, **2017**, 16(1), 132-138.
- [147] W. Luo, M. Sankar, A. M. Beale, Q. He, C. J. Kiely, P. C. A. Bruijninx, B. M. Weckhuysen, *Nat. Commun.*, **2015**, 6(1), 6540.

- [148] D. M. Alonso, S. G. Wettstein, J. A. Dumesic, *Chem. Soc. Rev.*, **2012**, *41*(24), 8075-8098.
- [149] Y. W. Chua, Y. Yu, H. Wu, *Fuel*, **2017**, *200*, 70-75.
- [150] C. A. Teles, P. M. de Souza, A. H. Braga, R. C. Rabelo-Neto, A. Teran, G. Jacobs, D. E. Resasco, F. B. Noronha, *Appl. Catal. B*, **2019**, *249*, 292-305.
- [151] P. Sirous-Rezaei, Y.-K. Park, *Chem. Eng. J.*, **2020**, *386*, 121348.
- [152] X. Hu, Z. Zhang, M. Gholizadeh, S. Zhang, C. H. Lam, Z. Xiong, Y. Wang, *Energy Fuels*, **2020**, *34*(7), 7863-7914.
- [153] Y. Li, C. Zhang, Y. Liu, S. Tang, G. Chen, R. Zhang, X. Tang, *Fuel*, **2017**, *189*, 23-31.
- [154] S. Echeandia, B. Pawelec, V. L. Barrio, P. L. Arias, J. F. Cambra, C. V. Loricera, J. L. G. Fierro, *Fuel*, **2014**, *117*, 1061-1073.
- [155] A. Al-Nayili, K. Yakabi, C. Hammond, *J. Mater. Chem. A*, **2016**, *4*(4), 1373-1382.
- [156] C. T. Campbell, *Acc. Chem. Res.*, **2013**, *46*(8), 1712-1719.
- [157] A. Kumar, A. Kumar, B. Biswas, J. Kumar, S. R. Yenumala, T. Bhaskar, *Renew. Energy*, **2020**, *151*, 687-697.
- [158] M. Besson, P. Gallezot, *Catal. Today*, **2003**, *81*(4), 547-559.
- [159] S. R. J. Saunders, M. Monteiro, F. Rizzo, *Prog. Mater. Sci.*, **2008**, *53*(5), 775-837.
- [160] A. J. Garcia-Olmo, A. Yopez, A. M. Balu, A. A. Romero, Y. Li, R. Luque, *Catal. Sci. Technol.*, **2016**, *6*(13), 4705-4711.
- [161] S. Hu, W. Li, *Science*, **2021**, *374*(6573), 1360-1365.
- [162] Z. Luo, G. Zhao, H. Pan, W. Sun, *Adv. Energy Mater.*, **2022**, *12*(37), 2201395.
- [163] A. A. Vedyagin, A. M. Volodin, R. M. Kenzhin, V. O. Stoyanovskii, Y. V. Shubin, P. E. Plyusnin, I. V. Mishakov, *Catal. Today*, **2017**, *293*, 73-81.
- [164] A. Vjunov, M. A. Derewinski, J. L. Fulton, D. M. Camaioni, J. A. Lercher, *J. Am. Chem. Soc.*, **2015**, *137*(32), 10374-10382.
- [165] S. Proding, M. A. Derewinski, *Pet. Chem.*, **2020**, *60*, 420-436.
- [166] L. Zhang, K. Chen, B. Chen, J. L. White, D. E. Resasco, *J. Am. Chem. Soc.*, **2015**, *137*(36), 11810-11819.
- [167] D. W. Gardner, J. Huo, T. C. Hoff, R. L. Johnson, B. H. Shanks, J.-P. Tessonnier, *ACS Catal.*, **2015**, *5*(7), 4418-4422.
- [168] T. Ennaert, J. Geboers, E. Gobechiya, C. M. Courtin, M. Kurttepel, K. Houthoofd, C. E. A. Kirschhock, P. C. M. M. Magusin, S. Bals, P. A. Jacobs, B. F. Sels, *ACS Catal.*, **2015**, *5*(2), 754-768.
- [169] S. Salakhum, K. Saenluang, C. Wattanakit, *Sustainable Energy Fuels*, **2020**, *4*(3), 1126-1134.
- [170] B. Gil, W. J. Roth, J. Grzybek, A. Korzeniowska, Z. Olejniczak, M. Eliáš, M. Opanasenko, J. Čejka, *Catal. Today*, **2018**, *304*, 22-29.
- [171] Y. Wang, P. Guerra, A. Zaker, A. R. Maag, G. A. Tompsett, L. J. Smith, X. Huang, J. Q. Bond, M. T. Timko, *ACS Catal.*, **2020**, *10*(12), 6623-6634.
- [172] J. Lu, J. W. Elam, and P. C. Stair, *Acc. Chem. Res.*, **2013**, *46*(8), 1806-1815.
- [173] N. Pino, T. Bui, G. Hincapié, D. López, Daniel E. Resasco, *Appl. Catal., A*,

2018, 559, 94-101.

[174] J. S. Bates, R. Gounder, *J. Catal.*, **2018**, 365, 213-226.

[175] M. J. Cordon, J. W. Harris, J. C. Vega-Vila, J. S. Bates, S. Kaur, M. Gupta, M. E. Witzke, E. C. Wegener, J. T. Miller, D. W. Flaherty, D. D. Hibbitts, R. Gounder, *J. Am. Chem. Soc.*, **2018**, 140(43), 14244-14266.

[176] H.-T. Vu, F. M. Harth, N. Wilde, *Front. Chem.*, **2018**, 6, 143.

[177] S. Prodingler, M. A. Derewinski, A. Vjunov, S. D. Burton, I. Arslan, Johannes A. Lercher, *J. Am. Chem. Soc.*, **2016**, 138(13), 4408-4415.

[178] P. A. Zapata, J. Faria, M. P. Ruiz, R. E. Jentoft, D. E. Resasco, *J. Am. Chem. Soc.*, **2012**, 134(20), 8570-8578.

[179] S. Prodingler, H. Shi, S. Eckstein, J. Z. Hu, M. V. Olarte, D. M. Camaioni, M. A. Derewinski, J. A. Lercher, *Chem. Mater.*, **2017**, 29(17), 7255-7262.

[180] J. Grand, S. N. Talapaneni, A. Vicente, C. Fernandez, E. Dib, H. A. Aleksandrov, G. N. Vayssilov, R. Retoux, P. Boullay, J.-P. Gilson, V. Valtchev, S. Mintova, *Nat. Mater.*, **2017**, 16(10), 1010-1015.